Journal of Steroid Biochemistry and Molecular Biology 211 (2021) 105904

Contents lists available at ScienceDirect

Journal of Steroid Biochemistry and Molecular Biology

journal homepage: www.elsevier.com/locate/jsbmb

Synthesis of dihydrotestosterone derivatives modified in the A-ring with (hetero)arylidene, pyrazolo[1,5-*a*]pyrimidine and triazolo[1,5-*a*] pyrimidine moieties and their targeting of the androgen receptor in prostate cancer

Márton A. Kiss [a,1], Miroslav Peřina [b,1], Václav Bazgier [c,d], Nóra V. May [e], Ádám Baji [a], Radek Jorda [b,*], Éva Frank [a,*]

[a] *Department of Organic Chemistry, University of Szeged, Dóm tér 8, Szeged, H-6720, Hungary*
[b] *Department of Experimental Biology, Faculty of Science, Palacký University Olomouc, Šlechtitelů 27, Olomouc, 78371, Czech Republic*
[c] *Department of Physical Chemistry, Faculty of Science, Palacký University Olomouc, Šlechtitelů 241/27, Olomouc, 77900, Czech Republic*
[d] *Laboratory of Growth Regulators, The Czech Academy of Sciences, Institute of Experimental Botany & Palacký University, Šlechtitelů 27, Olomouc, 78371, Czech Republic*
[e] *Centre for Structural Science, Research Centre for Natural Sciences, Magyar tudósok körútja 2, Budapest, H-1117, Hungary*

ARTICLE INFO

Keywords:
2-arylidene-dihydrotestosterone
Azolo[1,5-*a*]pyrimidines
Heterocyclization
Crystal structures
Androgen receptor
Flexible docking
Transcriptional activity

ABSTRACT

One of the main directions of steroid research is the preparation of modified derivatives in which, in addition to changes in physicochemical properties, receptor binding is significantly altered, thus a bioactivity different from that of the parent compound predominates. In the frame of this work, 2-arylidene derivatives were first synthesized by regioselective modification of the A-ring of natural sex hormone, 5α-dihydrotestosterone (DHT). After Claisen-Schmidt condensations of DHT with (hetero)aromatic aldehydes in alkaline EtOH, heterocyclizations of the α,β-enones were performed with 3-amino-1,2,4-triazole, 3-aminopyrazole and 3-amino-5-methylpyrazole in the presence of *t*-BuOK in DMF to afford 7′-epimeric mixtures of A-ring-fused azolo-dihydropyrimidines, respectively. Depending on the electronic demand of the substituents of the arylidene moiety, spontaneous or 2,3-dichloro-5,6-dicyanobenzoquinone (DDQ)-induced oxidation of the heteroring led to triazolo[1,5-*a*]pyrimidines and pyrazolo[1,5-*a*]pyrimidines in good yields, while, using the Jones reagent as a strong oxidant, 17-oxidation also occurred. The crystal structures of an arylidene and a triazolopyrimidine product have been determined by single crystal X-ray diffraction and both were found to crystallize in the monoclinic crystal system at $P2_1$ space group. Most derivatives were found to diminish the transcriptional activity of androgen receptor (AR) in reporter cell line. The candidate compound (17β-hydroxy-2-(4-chloro)benzylidene-5α-androstan-3-one, **2f**) showed to suppress androgen-mediated AR transactivation in a dose-dependent manner. We confirmed the cellular interaction of **2f** with AR, described the binding in AR-binding cavity by the flexible docking and showed the ability of the compound to suppress the expression of AR-regulated genes in two prostate cancer cell lines.

Abbreviations: 3AMP, 3-amino-5-methylpyrazole; 3AP, 3-aminopyrazole; 3AT, 3-aminotriazole; ATP, adenosine triphosphate; AR, androgen receptor; ARE, androgen response element; *n*-BuOH, normal butanol; *t*-BuOK, potassium *tert*-butylate; CETSA, cellular-thermal shift assay; CPPI, 3-(4-chlorophenyl)-6,7-dihydro-5*H*-pyrrolo[1,2-*a*]imidazole; CSS, charcoal stripped serum; CRPC, castration-resistant prostate cancer; CYP17A1, steroid 17α-hydroxylase/17,20-lyase; DCTA, *trans*-1,2-diaminocyclohexane-*N*,*N*,*N*′,*N*′-tetraacetic acid; DDQ, 2,3-dichloro-5,6-dicyanobenzoquinone; DHT, 5α-dihydrotestosterone; DMF, *N*,*N*-dimethylformamide; DTT, dithiotreitol; ESI-MS, electrospray ionization mass spectrometry; EtOH, ethanol; HMBC, heteronuclear multiple bond correlation; HSQC, heteronuclear single quantum correlation; LBD, ligand-binding domain; LHRH, luteinizing hormone-releasing hormone; MW, microwave; NOESY, nuclear overhauser effect spectroscopy; NMR, nuclear magnetic resonance; ORTEP, Oak Ridge Thermal-Ellipsoid Plot program for crystal structure illustrations; PARP, poly(ADP-ribose)polymerase; PBS, phosphate-buffered saline; PCR, polymerase chain reaction; PSA, prostate-specific antigen; RIPA, radioimmunoprecipitation assay buffer; SDS-PAGE, sodium dodecyl sulphate–polyacrylamide gel electrophoresis; TLC, thin layer chromatography.

* Corresponding authors.
E-mail addresses: radek.jorda@upol.cz (R. Jorda), frank@chem.u-szeged.hu (É. Frank).
[1] These authors contributed equally to this work.

https://doi.org/10.1016/j.jsbmb.2021.105904
Received 18 March 2021; Received in revised form 20 April 2021; Accepted 27 April 2021
Available online 29 April 2021

1. Introduction

The androgen receptor (AR) is a ligand-activated transcription factor that belongs to the superfamily of steroid and thyroid hormone receptors and plays a crucial role in the normal development of male reproductive tissues. High expression and/or relaxation of AR regulation is strongly implicated in prostate cancer (PCa). Current therapeutic strategies for the treatment of PCa include androgen deprivation and radiation therapy (*e.g.* anti-LHRH agents), surgery, chemotherapy (*e.g.* docetaxel, cabazitaxel) or the use of steroidal (*e.g.* abiraterone) or non-steroidal antiandrogens (*e.g.* enzalutamide) (Fig. 1) or PARP inhibitors [1]. Unfortunately, the disease rapidly progresses to castration-resistant prostate cancer (CRPC) stage, which is defined by AR-pathway alterations including AR gene amplification, overexpression, mutation, splice variants, and the increase in adrenal and intratumoral androgens.

AR splicing variants [2], which lack the ligand-binding domain as a result of alternative splicing of the AR gene, are emerging as a crucial mechanism in CRPC progression. Among these variants, AR-V7 is the most clinically meaningful and the most frequently expressed receptor variant in PCa samples [3]. Several anti-AR-V7 strategies have been described, including inhibition of the transcription of the AR gene, inhibition of splicing to generate AR-V7, destabilization of the AR-V7 transcript and protein, AR degradation, blocking of AR synthesis, inhibition of the constitutive activity of AR-V7 in the nucleus, interference with intracellular trafficking of AR, and inhibition of downstream signalling related to AR-V7 activation [4,5].

Several steroidal compounds, mostly modified in the D-ring of the androstane core have been investigated as AR modulators or for their anti-PCa properties [6–11], but only galeterone [12] and abiraterone [13] (Fig. 1) have entered clinical trials. Both agents showed to target adrenal and tumour androgen production by inhibition of the steroidogenic enzyme CYP17A1, and galeterone is capable to induce AR and AR-V7 degradation in PCa by competitive antagonism of AR [14]. In the clinic, galeterone is shown to be well tolerated and demonstrates pharmacodynamic changes consistent with its selective, multifunctional AR signaling inhibition [15]. Unfortunately, recent results from phase 3 clinical trials on AR-V7 and metastatic CRPC patients have not confirmed galeterone's efficacy [16]. In addition, the fact that abiraterone-treated patients generally relapse within one year indicated the resistance mechanism to abiraterone that is accompanied by upregulation of CYP17A1 and induction of AR and AR splice variants [2,17]. For the above reasons, investigations of other ligands are desirable.

We previously described several D-ring-attached steroidal azoles, structurally similar to abiraterone, displaying CYP17A1 inhibitory effect [18–20]. Recently, some A-ring-fused arylpyrazoles [21] and arylpyrimidines [22] of 5α-dihydrotestosterone (DHT) have also been demonstrated to exert anticancer activity against multiple cancer cell lines including PCas. Some recent articles reported steroidal compounds with pyrazolo[1,5-*a*]pyrimidine and triazolo[1,5-*a*]pyrimidine moieties [23, 24] but without deeper pharmacological investigations. In the current work, additional A-ring-modified derivatives of DHT containing (hetero)arylidene, pyrazolo[1,5-*a*]pyrimidine and triazolo[1,5-*a*]pyrimidine moieties have been synthesized and their ability to affect the transcriptional activity of AR in reporter cell line was investigated. Structural determination of all compounds was accomplished by ^{1}H and ^{13}C NMR spectroscopy and electrospray ionization mass spectrometry (ESI-MS), while for two representative molecules, by single crystal X-ray diffraction. Candidate compound was further studied and showed to interact with AR and to suppress expression of Nkx3.1 and PSA in PCa. Finally, interaction within the AR's cavity was performed by the flexible docking.

2. Results and discussion

2.1. Synthesis and characterization of the target compounds

As a first synthetic modification, DHT was reacted with benzaldehyde (**1a**), substituted benzaldehydes **1b**–**h** and heteroaromatic aldehydes **1i** and **1j**, respectively, in order to obtain 2-(hetero)arylidene-3-ones **2a–j** suitable for cyclization with binucleophilic reagents (Table 1, entries 1–12). Arylaldehydes were selected to ensure that their reactivity covered a wide spectrum, *i.e.* in addition to benzaldehyde **1a**, derivatives containing both electron donating (CH_3 and OMe) and electron withdrawing groups (Cl, CN, NO_2) were used. The synthesis of a structurally related 2-methylidene derivative **2k** from DHT with excess acetaldehyde **1k** has been reported previously [21] (Table 1, entry 13).

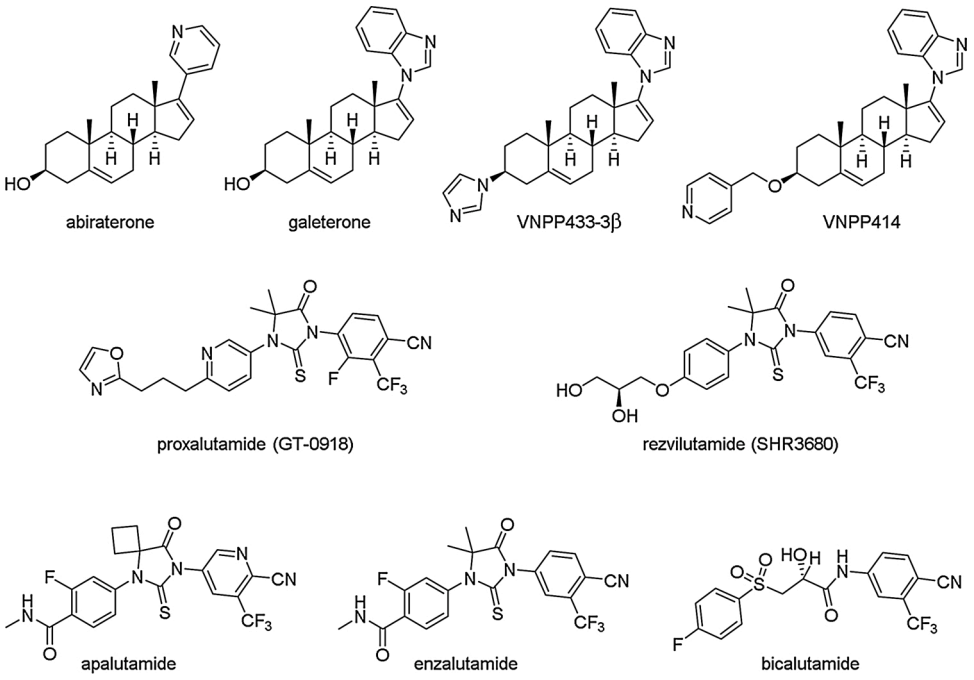

Fig. 1. Representatives of steroidal and non-steroidal anti-PCa agents, which reduce endogenous androgen production by the inhibition of CYP17A1 and/or act as AR antagonists.

Table 1
Synthesis of A-ring-modified α,β-enones **2a**–**k** from DHT.

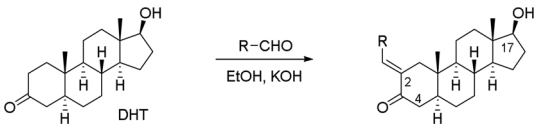

Entry	R-CHO [a]	R	Temperature (°C)	Time	Product	Yield (%) [b]
1	**1a**	Ph	reflux	30 min	**2a**	74
2	**1a**	Ph	r.t.	3 h	**2a**	92
3	**1a**	Ph	80 (MW)	10 min	**2a**	69
4	**1b**	*p*-$CH_3C_6H_4$	r.t.	4 h	**2b**	87
5	**1c**	*m*-$CH_3C_6H_4$	r.t.	4 h	**2c**	89
6	**1d**	*p*-MeO-C_6H_4	r.t.	4 h	**2d**	89
7	**1e**	*p*-F-C_6H_4	r.t.	3 h	**2e**	91
8	**1f**	*p*-Cl-C_6H_4	0	3 h	**2f**	90
9	**1g**	*p*-CN-C_6H_4	0	1 h	**2g** [c]	–
10	**1h**	*p*-$NO_2C_6H_4$	0	1 h	**2h** [c]	–
11	**1i**	furan-2-yl	0	3 h	**2i**	84
12	**1j**	tiophen-2-yl	0	3 h	**2j**	83
13	**1k**	CH_3	−10	3.5 h	**2k** [d]	70

[a] 1.2 equiv.
[b] After purification by column chromatography.
[c] In addition to compound **2**, the significant formation of the 4-arylidene and 2,4-diarylidene derivatives were detected.
[d] The synthesis has been reported previously [21].

Although Claisen-Schmidt condensation of arylaldehydes to the C16 position of 17-ketosteroids was found to lead to the corresponding D-ring substituted products in alkaline EtOH both at room temperature [25] and under reflux [26], in the case of the A-ring, a regioselectivity problem may arise from the two α-carbon atoms (C2 and C4) adjacent to the C3 carbonyl group available for substitution. The reaction conditions may vary depending on the different electronic nature and thus reactivity of the aldehydes used.

For a preliminary experiment, the reaction of DHT and benzaldehyde **1a** in 1:1.2 M ratio was carried out in alkaline EtOH at both reflux and room temperatures (r. t.). Although at 25 °C longer time (3 h) was needed than in boiling EtOH (30 min) for complete conversion, the selectivity was found to be better, and the 2-benzylidene derivative **2a** was obtained selectively in excellent yield (94 %, Table 1, entry 1). Higher temperature (entry 2) and especially microwave (MW) irradiation (80 °C, 10 min, entry 3) favoured the formation of the 4-isomer as an undesired by-product.

During the Claisen-Schmidt condensation of DHT performed with other arylaldehydes **1b**–**h**, the reaction rates were found to be affected significantly by the different R substituents in the aromatic ring. Longer reaction time (4 h) at room temperature was needed for the regioselective formation of the desired products **2b**–**d** in cases of arylaldehydes **1b–d** containing electron donating groups (CH_3, OMe), which can be explained by the decreased electrophilicity of these reagents (Table 1, entries 4–6). While *p*-fluorobenzaldehyde (**1e**) displayed similar reactivity to benzaldehyde (entry 7), a lower temperature was required to achieve adequate regioselectivity when **1f** with an electron-withdrawing Cl atom or heteroaryl aldehydes (**1g**, **1h**) were used, due to the higher reactivity of these carbonyl compounds. It is also important to note that arylaldehydes **1g** and **1h** having a strong electron-withdrawing group (CN or NO_2) were so reactive even at low temperature that the transformations resulted in the inseparable mixtures of 2- (**2g** or **2h**) and 4-arylidene derivatives as well as 2,4-disubstituted products (entries 9 and 10), therefore these reactions were abandoned.

The structure of the novel arylidene (**2a**–**f**) and heteroarylidene derivatives (**2i** and **2 j**) in solution was confirmed by ^{1}H and ^{13}C NMR measurements, which indicated the presence of the characteristic signals of the aromatic ring from the aryl- and heteroarylaldehydes (Supplementary Material, S1-S30). Since the usually more stable and thus favoured (*E*)-configuration along the double bond was earlier evidenced by NOESY correlations between the 1-H and 21-CH_3 protons for **2k** [21], the same stereochemistry in solution appears to be certain for the structural analogues (**2a–f**, **2i**, **2j**) containing a larger (hetero)aromatic ring than the CH_3 group of **2k**.

The solid phase structure of **2a** was determined by single crystal X-ray diffraction. The molecule crystallized in the monoclinic crystal system in $P2_1$ space group. ORTEP representation together with atom numbering of the compound and the packing arrangements viewed from the crystallographic direction 'a' is depicted in Fig. 2. The unit cell, containing two molecules, is shown in **Fig. S1** and the packing arrangements viewed from the 'a', 'b' and 'c' crystallographic directions are shown in **Fig. S2**. The torsion angle measured for C2-C26-C1′-C6′ was found to be 16.5° showing that the phenyl ring is in a plane with the DHT rings. Bond distances and angles are collected in **Tables S1** and **S2**. The molecules are arranged in columns by the help of O2-H2O…O1 connection between neighboring molecules (**Fig. S3**). Some selected hydrogen bond data is shown in **Table S3**. Because of the steric hindrance of the C18 and C19 methyl groups, the molecules above each other are shifted away and C4-H4A…π and C5-H5…π secondary interactions are forming between C–H protons and the phenyl rings (**Fig. S3**). The crystal does not contain any solvent accessible voids.

As a continuation, the ring-closure reactions of the synthesized steroidal α,β-enones with different aminoazole reagents were planned to carry out. The initial experiments were performed with the benzylidene derivative **2a**, in order to find the optimum conditions for the synthesis of pyrazolo[1,5-*a*]pyrimidines and triazolo[1,5-*a*]pyrimidines (Scheme 1). Although *t*-BuOK has often been used as catalyst in polar protic solvents, such as EtOH or *n*-BuOH, for similar heterocyclizations of α,β-unsaturated ketones, long reaction times (6–30 h) under reflux were generally required for complete conversions [23,27]. Since the progress of the reaction of **2a** with 3-amino-5-methylpyrazole (3AMP), 3-aminopyrazole (3AP) or 3-aminotriazole (3AT) also proved to be very slow under these conditions, MW irradiation was first applied to obtain rate acceleration. In the latter cases, however, the formation of a significant amount of by-products was observed. As a next attempt, EtOH was replaced with DMF in the presence of *t*-BuOK, which in each case led to almost complete conversion indicated by a sharp colour change of the mixtures, within 45 min at 140 °C (Scheme 1). The same reactions in DMF required 3 h when KOH was used as a base. TLC monitoring confirmed the formation of two new substances in each reaction. The NMR spectroscopic analysis showed that the less polar compounds were the target products **6a**–**8a**, while the more polar molecule proved to be

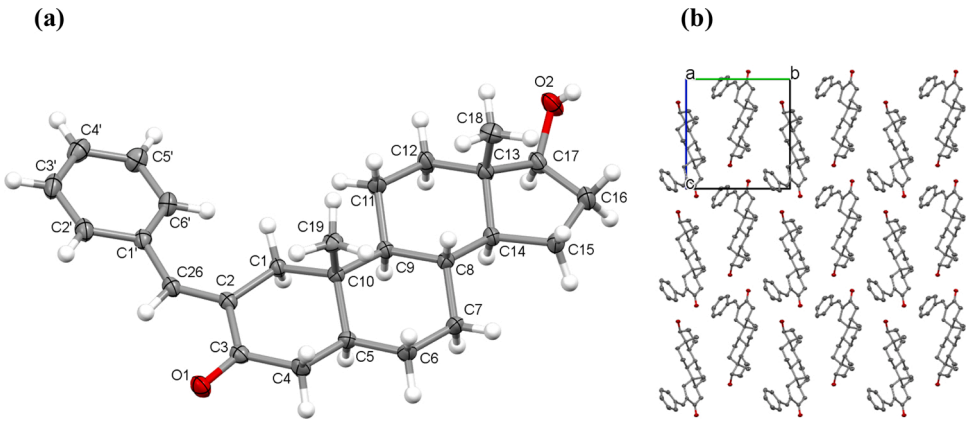

Fig. 2. Crystal structure of **2a** showing the (**a**) ORTEP representation of the molecule with atom numbering (displacement parameters are drawn at 50 % probability level) and (**b**) the packing arrangement of the molecules (without hydrogen atoms) viewed from crystallographic direction 'a'.

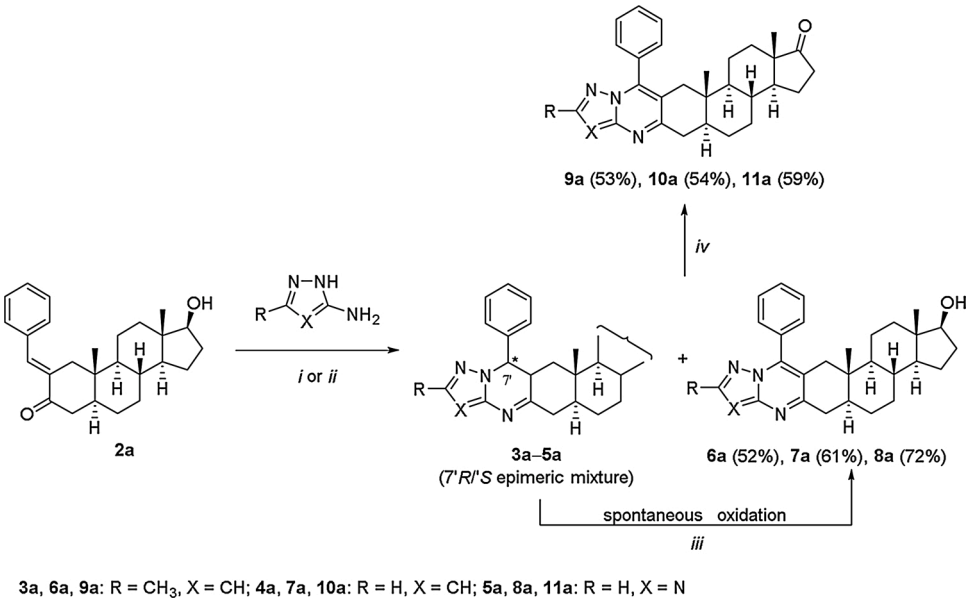

Scheme 1. Synthesis of pyrazolo[1,5-*a*]pyrimidines and triazolo[1,5-*a*]pyrimidines from 2-benzylidene derivative (**2a**) of DHT. *Reagents and conditions*: Azoles: 3AMP (R = CH_3, X = CH), 3AP (R = H, X = CH), 3AT (R = H, X = N); (*i*) *t*-BuOK, DMF, 140 °C, 45 min; (*ii*) KOH, DMF, 140 °C, 3 h; (*iii*) stirred in air, 25 °C, 24 h; (*iv*) Jones reagent, acetone, r.t., 30 min..

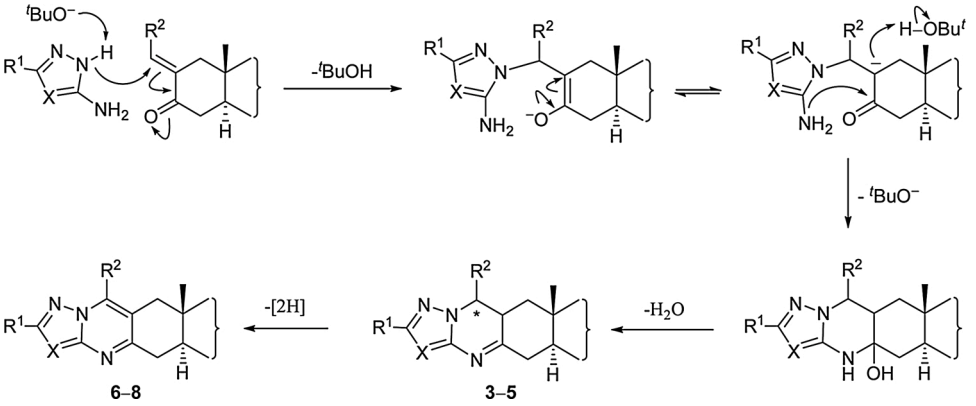

Fig. 3. Proposed mechanism for the formation of azolo[1,5-*a*]pyrimidines.

its unoxidized precursor as an inseparable mixture of two epimers **3a**–**5a**. Since the autooxidation also occurred during the reaction, the reaction mixtures were stirred for an additional 24 h at room temperature after conversion of the benzylidene derivative **2a** in order to complete the oxidation to **6a**–**8a**. The yields of the desired products were found to be the highest (**8a**, 72%) when 3AT was used for the cyclization, while only moderate yield (**6a**, 52 %) was obtained in case of 3AMP. During the reactions with pyrazole reagents, small amounts of unconverted starting material **2a** were also detected, suggesting the lower reactivity of these reagents compared to 3AT. Nevertheless, according to the TLC monitoring of the reaction mixtures, the moderate yields were not justified unless the formation of some polar by-product adhering to the silica gel reduced the yield of the desired compounds.

The presumed mechanism may provide an answer to the experimental findings (Fig. 3). Since the azole reagents are very weak acids, a strong base is needed (KOH or *t*-BuOK) to deprotonate the ring-N atom, so that the *aza*-Michael addition to the enone can occur more efficiently. The increase in reaction rate by using *t*-BuOK in a polar aprotic (DMF) instead of a polar protic solvent (EtOH or *n*-BuOH) can be explained by the higher basicity of *t*-BuOK under this condition, as the solvent can interact only with the potassium centre. The isolated yields of the desired products can be affected by the acidic strength of the azoles, as well as the tendency of the polar intermediate formed by heterocyclization to lose water (Fig. 3). The latter compound can reduce the yield of the azolo[1,5-*a*]pyrimidines as highly polar by-product.

In contrast to the spontaneous oxidation of the heterocyclic moiety of **3a**–**5a**, complete oxidation of the crude products with the Jones reagent in acetone affected both the dihydropyrimidine ring and the 17−OH group, and resulted in the corresponding heteroaromatic 17-keto derivative **9a**–**11a** in moderate yields (Scheme 1).

It is important to note that a one-pot three-component reaction of DHT, benzaldehyde (**1a**), and 3AP was also attempted [28], but these types of reactions were discarded due to long reaction times, purification difficulties, and similar product yields. The fact that α,β-enone intermediates may also be of pharmacological interest also supported the stepwise pathway.

Since the highest product yield was obtained when 3AT was applied for heterocyclization, the other (hetero)arylidene derivatives (**2b**–**f**, **2i**, **2j**) were converted to A-ring-fused triazolo[1,5-*a*]pyrimidines only using this reagent under the previously optimized conditions. According to the experimental results summarized in Table 2, in most of the cases the cyclization and subsequent spontaneous oxidation led to the desired products (**8b**–**e**, **8i**–**k**) in good yields (entries 1–4 and 6–8). However, 2,3-dichloro-5,6-dicyano-1,4-benzoquinone (DDQ) was required as mild oxidizing agent to convert **5f** (Fig. 3), which contains an electron-withdrawing Cl atom on the benzene ring, to **8f** (entry 5). DDQ could also be used for other derivatives to accelerate the heteroaromatization, as oxidation occurred rapidly in dioxane under MW irradiation at 120 °C within 5 min. When the product mixture containing **5** and **8** of each reaction was treated with the Jones reagent as strong oxidizing agent, not only the dihydropyrimidine ring but also the 17β-hydroxyl group was oxidized to a ketone to give derivatives **11** (Table 2).

The structure of all heterocyclic products was confirmed by 1D and 2D NMR as well as ESI-MS measurements. A comparison of the proton spectra of the 17−OH (**6a**, **7a**, **8**) and 17-keto derivatives (**9a**, **10a**, **11**) showed that the proton peaks of the angular C18 and C19 methyl groups were interchanged. Since 19-H_3 is in similar chemical environment for all compounds, the location of its peak does not change significantly, however, for 17-ones, the 18-H_3 protons are deshielded due to the strong electron-attracting effect of the carbonyl group, so that the singlet signal corresponding to these equivalent protons appears at a higher chemical shift. It can also be attributed to the presence of the carbonyl group in compounds **9a**, **10a** and **11**, that the multiplet peaks of the 16-H_2 protons are shifted downfield (2.08 and 2.45 ppm), separately from the signals of the other backbone protons. In the aliphatic region of the spectra, proton signals belonging to C1 and C4 with characteristic splitting can be observed. While the signals of 1-H_2 appear as two doublets with the same coupling constant due to the germinal coupling, 4-H_2 gives two double doublet peaks because of both geminal coupling and coupling to a single proton on the adjacent C5 carbon atom. The spectrum of compounds **9a**, **10a** and **11** lacks the triplet of the 17-H proton characteristic of derivatives **6a**, **7a** and **8**, which proves that oxidation has occurred. The aromatic region of the spectrum of all compounds shows the signals of the protons on the pyrimidine ring, as well as a singlet of 2′-H for triazole derivatives **8** and **11**, two intercoupling doublets of the 2′-H and 3′-H for unsubstituted pyrazoles **7a** and **10a** and a singlet of 3′-H for methylpyrazoles **6a** and **9a**. ^{1}H–^{13}C correlations were performed based on 2D NMR measurements (HSQC and HMBC) of one representative of each pyrazolopyrimidine (**7a**) and triazolopyrimidine derivative (**8a**) (Supplementary Material, S-11 and S-13). It should be noted that for some derivatives, certain carbon atoms belonging to the condensed heterocycle were observed as weak signals in the ^{13} C NMR (J MOD) spectra in spite of the high number of scans, presumably due to the long relaxation time of these carbon nuclei.

Crystal structure of **8j** was determined by single crystal X-ray diffraction. The molecule crystallized in the monoclinic crystal system in $P2_1$ space group and the asymmetric unit contains two molecules and one dichloromethane solvent molecule. ORTEP representation together with atom numbering of the compound and the packing arrangements viewed from the crystallographic direction 'a' is depicted in Fig. 4. The

Table 2
Synthesis of A-ring-fused triazolo[1,5-*a*]pyrimidines of DHT.

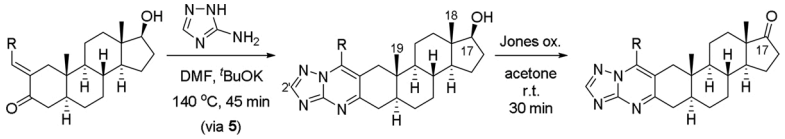

Entry	Enone	R^1	17-OH product	Yield (%) [b]	17=O product [c]	Yield (%) [b]
1	**2b**	*p*-$CH_3C_6H_4$	**8b**	76	**11b**	62
2	**2c**	*m*-$CH_3C_6H_4$	**8c**	77	**11c**	66
3	**2d**	*p*-MeO-C_6H_4	**8d**	71	**11d**	59
4	**2e**	*p*-F-C_6H_4	**8e**	73	**11e**	57
5	**2f** [a]	*p*-Cl-C_6H_4	**8f**	65	**11f**	62
6	**2i**	furan-2-yl	**8i**	59	**11i**	55
7	**2j**	thiophen-2-yl	**8j**	62	**11j**	57
8	**2k** [d]	CH_3	**8k**	69	**11k**	52

[a] After the heterocyclization, DDQ was used to oxidize the heteroring.
[b] After chromatographic purification.
[c] Jones oxidation was performed not with the purified **8**, but with the crude product containing both **5** and **8**, of the heterocyclization.
[d] Ref [21].

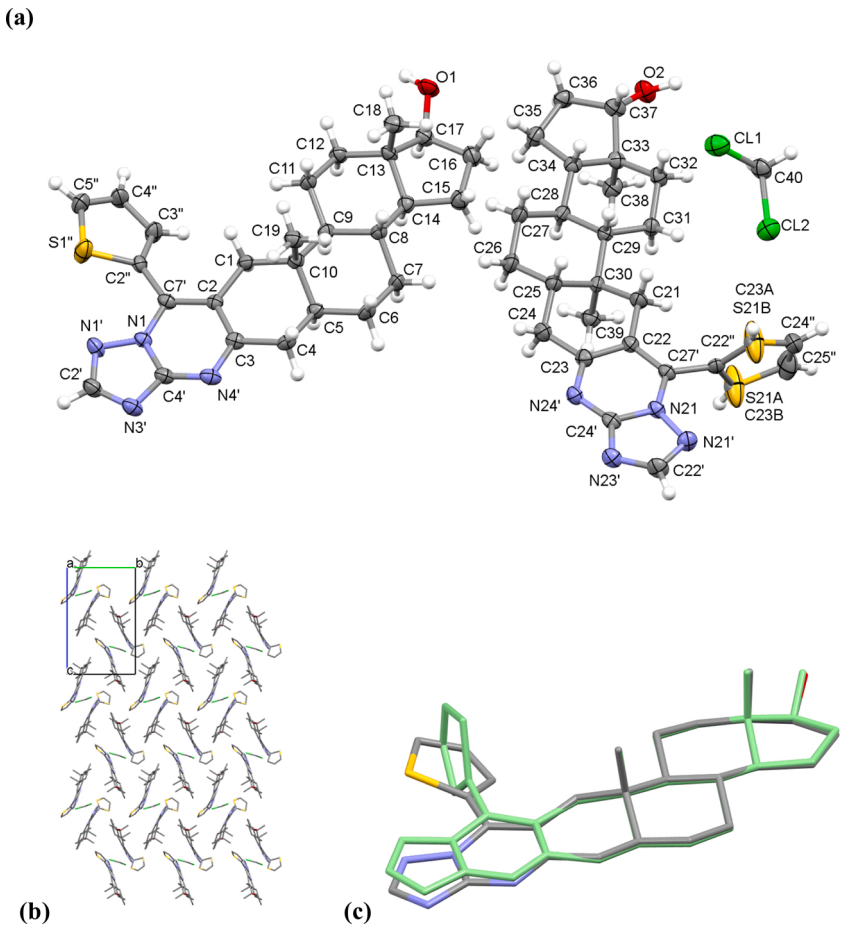

Fig. 4. Crystal structure of **8 j** showing the (**a**) ORTEP representation of the asymmetric unit with atom numbering (displacement parameters are drawn at 50 % probability level) and the (**b**) packing arrangement of the molecules (without hydrogen atoms) viewed from crystallographic direction 'a' and (**c**) overlay of the two molecules of the asymmetric unit (molecule 1 is coloured by element and molecule 2 is green).

unit cell containing four molecules is shown in **Fig. S4**, and the packing arrangements viewed from the 'a', 'b' and 'c' crystallographic directions are shown in **Fig. S5**. The two molecules of the asymmetric unit have different conformations. Overlay of the two structures in Fig. 4c clearly shows the different thiophene ring positions. Angles between thiophene and pyrimidine ring planes are 30.86° for molecule 1 and 83.47° for molecule 2. In case of molecule 2, the thiophene ring was found in two disordered position where the S21 and C23 atoms are interchanged. The occupancy of the major component containing C23A and S21A was found to be 76 %, while the minor component containing C23B and S21B atoms is 24 %. The rotational freedom of this ring is due to the fact that it interacts only from one direction with a neighbour by C24″-H24″…O1, while this freedom was not found for molecule 1 where the thiophene ring is involved in two hydrogen bonds with C5″-H5″…O2 and C4″-H4″….Cl1 (**Fig. S6** and **Table S3**). Selected bond distances and angles are collected in **Tables S1** and **S2**. The packing of the molecules arranged by hydrogen bonds is shown in **Fig. S3** and the data of the secondary interactions are collected in **Table S3**. The dichloromethane molecules are placed in voids of 72.2 $Å^3$, which is 2.9 % of the unit cell volume.

2.2. The effect of steroids on AR transcriptional activity and viability of PCa cells

AR modulators are known to influence AR-dependent transcription; therefore, we examined the metribolone (R1881)-stimulated transcriptional activity of AR after 24 h treatment with our novel DHT-derivatives. Compounds were screened at three concentrations using an AR-dependent reporter cell line, 22Rv1-ARE14, which was transfected with a reporter plasmid containing androgen response element (ARE) sequence and luciferase sequence [29].

The analysed library of novel A-ring modified DHT-derivatives comprised 9 α,β-enones (series **2**), 18 triazolo[1,5-*a*]pyrimidines (series **8** and **11**), and 4 pyrazolo[1,5-*a*]pyrimidines (**6a**, **7a**, **9a**, and **10a**). As shown in Table 3, α,β-enones from series **2** belong to the most active compounds (6 compounds reduced R1881-stimulated AR transactivation to 50 % at 10 μM concentration) with *p*-chlorobenzylidene derivate **2f** being the most potent steroid, whereas thiophene-2-yl derivative **2j** and ethylidene derivative **2k** belong to the least potent α,β-enones. DHT-derivatives from other series were active only partially (9 compounds reduced activity to 75 % of control) and only 3 members (**8k**, **11k**, and **11i**) were completely inactive. It is obvious that heterocyclization of **2a** with 3AT reduced the antiandrogenic effect (**8a**). We also observed that the methylation of the pyrazolo[1,5-*a*]pyrimidine **7a** resulted in the less active derivative **6a**. The same tendency displayed also 17-keto pairs of pyrazolo[1,5-*a*]pyrimidines **9a** and **10a.** The antagonistic activity of compounds **2f** (IC_{50} = 3.54 μM) and **2a** (IC_{50} = 6.92 μM) reached up to single-digit micromolar values and showed to be comparable with values obtained for standards, *i.e.* galeterone (IC_{50} = 5.82 μM) and enzalutamide (IC_{50} = 1.50 μM) (Supplementary Material, S38-S41).

Antiproliferative properties of all novel steroids were tested in two AR-positive PCa cell lines (22Rv1-ARE14, C4-2), both originated from metastatic lesions. Resulting data are presented as residual viability at 10 μM compounds after 72 h of treatment compared to untreated control. Antiproliferative activities of the most potent derivative **2f**

Table 3
AR antagonistic activity and antiproliferative activity of novel DHT-derivatives.

	Compound	Transcriptional AR activity (% ± SD) in 22Rv1-ARE14 after 24 h treatment[a]			Viability (% ± SD, 10 μM) after 72 h[b]	
		10 μM	2 μM	0.4 μM	22Rv1-ARE14	C4-2
α,β-enones C17-OH group	**2k**	67.0 ± 3.9	98.2 ± 3.0	>100	> 100	87.0 ± 1.9
	2a	36.4 ± 5.3	69.9 ± 0.9	81.3 ± 10.3	92.9 ± 1.1	92.8 ± 4.2
	2b	42.2 ± 5.6	73.6 ± 7.0	90.1 ± 7.9	91.2 ± 1.2	97.2 ± 2.8
	2c	49.3 ± 3.5	89.2 ± 2.7	100.0 ± 1.9	90.3 ± 1.9	> 100
	2d	38.9 ± 1.9	70.2 ± 5.5	91.0 ± 2.9	91.3 ± 1.9	93.7 ± 2.7
	2e	64.9 ± 4.2	86.1 ± 9.7	99.1 ± 9.9	80.2 ± 3.3	98.9 ± 2.2
	2f	34.2 ± 6.5	86.3 ± 4.6	>100	42.2 ± 12.8	74.0 ± 13.6
	2i	40.6 ± 7.3	78.7 ± 5.5	93.9 ± 9.1	> 100	91.9 ± 2.0
	2j	77.5 ± 8.7	>100	>100	> 100	57.4 ± 2.0
	8k	>100	>100	>100	87.5 ± 2.6	> 100
triazolo[1,5-*a*]pyrimidines C17-OH group	**8a**	77.6 ± 2.2	89.5 ± 3.0	91.2 ± 3.9	76.7 ± 1.3	93.5 ± 1.3
	8b	77.6 ± 3.0	86.1 ± 8.4	97.4 ± 4.0	70.8 ± 1.5	92.1 ± 1.9
	8c	86.1 ± 2.4	>100	>100	93.3 ± 1.2	94.2 ± 1.9
	8d	76.9 ± 1.5	91.6 ± 3.0	99.5 ± 4.8	91.1 ± 0.8	92.7 ± 1.6
	8e	86.7 ± 8.1	98.7 ± 2.2	98.1 ± 3.6	90.5 ± 2.1	88.4 ± 0.6
	8f	65.8 ± 5.2	94.3 ± 6.4	95.7 ± 4.1	94.1 ± 1.7	87.1 ± 4.0
	8i	67.1 ± 8.9	86.6 ± 3.7	97.9 ± 8.2	> 100	99.9 ± 2.5
	8j	59.9 ± 6.6	80.5 ± 8.6	97.5 ± 11.1	94.0 ± 2.2	90.9 ± 1.1
triazolo[1,5-*a*]pyrimidines C17-keto group	**11k**	>100	96.7 ± 7.2	95.6 ± 8.3	> 100	97.1 ± 2.3
	11a	86.9 ± 6.7	87.0 ± 1.8	90.0 ± 9.9	96.9 ± 0.3	100.0 ± 3.6
	11b	68.7 ± 2.1	84.0 ± 7.2	100.4 ± 5.6	93.7 ± 1.8	97.3 ± 7.4
	11c	75.0 ± 4.6	82.0 ± 10.1	91.3 ± 0.5	88.6 ± 1.0	99.6 ± 3.6
	11d	74.2 ± 1.7	81.2 ± 2.8	84.6 ± 0.6	93.3 ± 1.9	96.5 ± 3.9
	11e	93.1 ± 9.7	96.5 ± 2.1	98.3 ± 8.4	> 100	> 100
	11f	67.8 ± 2.4	85.3 ± 2.7	96.7 ± 1.1	90.5 ± 0.8	97.3 ± 2.5
	11i	>100	>100	>100	100.3 ± 2.0	99.7 ± 5.2
	11 j	88.6 ± 4.4	99.4 ± 7.4	>100	92.5 ± 1.0	> 100
pyrazolo[1,5-*a*] pyrimidines	**6a**	86.3 ± 4.4	>100	>100	> 100	99.1 ± 1.2
	7a	69.9 ± 2.5	>100	>100	> 100	99.7 ± 1.5
	9a	82.2 ± 1.7	>100	>100	> 100	> 100
	10a	62.5 ± 4.8	92.1 ± 6.6	>100	> 100	> 100
	Enzalutamide	14.3 ± 0.9	42.7 ± 2.2	75.4 ± 1.5	94.5 ± 1.2	90.0 ± 2.1
	Galeterone	34.6 ± 2.3	73.4 ± 2.9	92.4 ± 4.4	> 100	> 100

[a] Transcriptional activity normalized to signal of 1 nM R1881 = 100 %, measured at least in triplicate.
[b] Viability of treated cells normalized to the viability of control cell treated with vehicle, measured at least in triplicate.

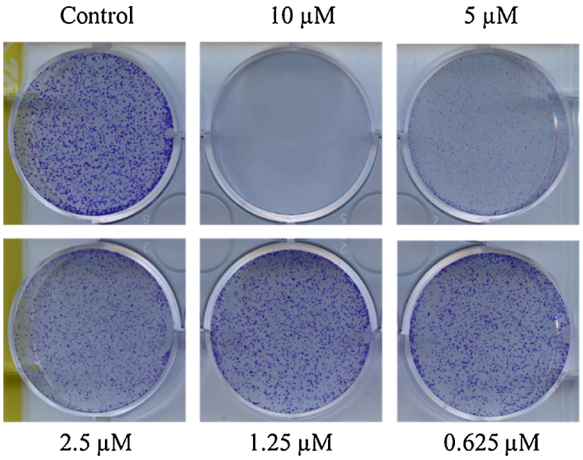

Fig. 5. Colony formation assay of 22Rv1-ARE14 PCa cells. Cells were treated with indicated concentrations of **2f** for 10 days. Medium was replaced by fresh medium with compound after 5 days. Representative result from two replicates is shown.

displayed mid-micromolar values (GI_{50} = 9.9 ± 1.8 μM and 15.7 ± 4.4 μM) in 22Rv1-ARE14 and C4-2, respectively. Compound **2f** showed to have higher antiproliferative activity than used standards with GI_{50} > 50 μM (Supplementary Material, S42-S47).

The prolonged antiproliferative effect of **2f** was further evaluated by clonogenic assay in 22Rv1-ARE14 cells. As shown in Fig. 5, **2f** is able to significantly inhibit formation of cell colonies in a dose dependent manner after 10 days of treatment.

2.3. *Effect of **2f** on the stability of AR and its cellular localization*

Previous findings showed that steroidal agonists (testosterone, DHT and R1881) can induce thermal stabilisation of AR performed by cellular-thermal shift assay (CETSA) [30]. This technology was previously found to confirm binding of nonsteroidal AR-antagonists CCPI and enzalutamide [30,31], therefore we performed this assay for **2f** (Fig. 6). In control experiment, the incubation of C4-2 cells with 100 nM R1881 confirmed previously published increase in thermal stability of AR [30]. Similar results were obtained with multiple concentrations of **2f** that, in our opinion, originate from more extensive interaction with AR-LBD.

The AR becomes strongly concentrated in the nucleus in response to androgens [32] where it drives the transcription of target genes. Several AR modulators showed to block the transport and accumulation of AR to nucleus [33–35] as a result of its targeting. Therefore, we investigated the effect of **2f** on AR distribution in R1881-stimulated cells. As shown in Fig. 7, **2f** and galeterone markedly decreased the transport of AR to the nucleus in comparison to androgen-activated cells. While AR remained in cytosol upon the treatment of cells with **2f**, galeterone induced also partial AR degradation (see densitometric analysis).

2.4. *Molecular docking of DHT derivative **2f** to AR-LBD*

The AR contains a narrow nonpolar active site with two hydrogen-bonding capacities: arginine (R752) towards carbonyl group on the A-ring, while threonine (T877) and asparagine (N705) towards the hydroxyl group on the D-ring of DHT. To confirm the location of ligand **2f** within the AR's cavity, the flexible docking study was performed [10]. Very importantly, candidate compound **2f** showed similar interactions with AR binding site as DHT. This basic motif allows binding of **2f** to the

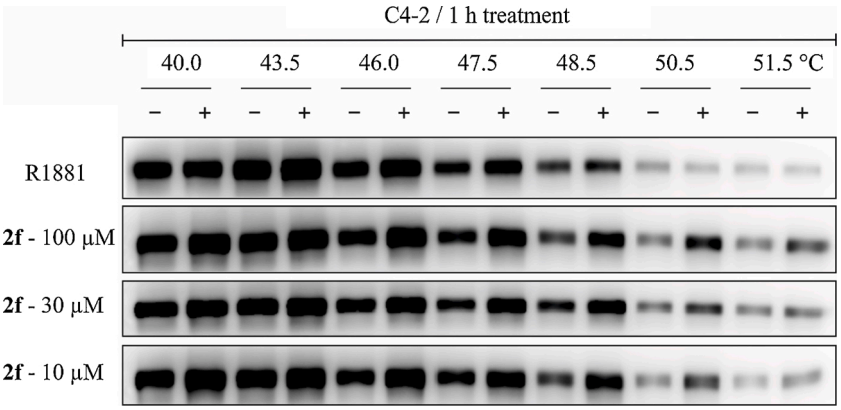

Fig. 6. Western blots showing protein level of AR (soluble fraction) after indicated heat shocks of C4-2 cells after 1 h treatment in absence (-) or presence (+) of 100 nM R1881 or **2f** in different concentrations.

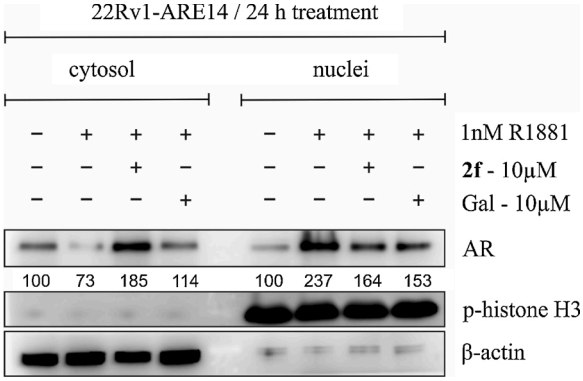

Fig. 7. Western blotting analysis showing AR distribution in 22Rv1-ARE14 cells. The cells were cultivated in CSS medium for 24 h and then treated with 1 nM R1881 alone or in combination with **2f** or galeterone (Gal) for additional 24 h. Cellular fractions were isolated using the Qproteome Cell Compartment Kit (Qiagen) and subjected for immunoblot analysis of appropriate proteins. Phosphorylated histone H3 and β-actin levels were used as controls of equal protein loading and quality of separation, respectively. Quantification was performed using Multigauge 3.0 software. Representative result from two replicates is shown.

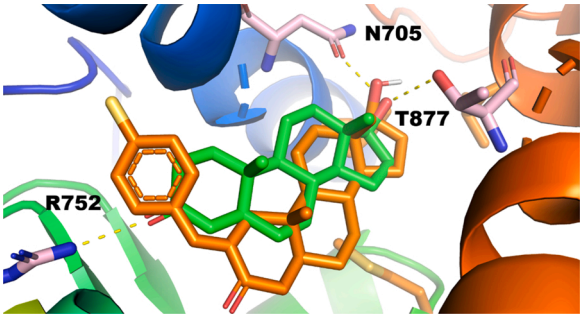

Fig. 8. Detailed view of the active site of the AR (PDBID:2PIV) with DHT as natural ligand (green compound, binding energy dG -10.9 kcal/mol) and candidate compound **2f** (orange, binding energy dG Vina -12.7 kcal/mol). Hydrogen bonds (depicted as yellow dashed lines) can be observed between compound **2f** and amino acids N705 and T877, similarly to DHT, that also makes the hydrogen bond with the amino acid R752.

same hydrogen bonds to arginine (R752) and asparagine (N705) as template (Fig. 8). Candidate compound **2f** showed stronger binding energy (dG Vina - –12.7 kcal/mol,) in comparison with the natural ligand DHT (dG Vina -10.9 kcal/mol).

*2.5. Effects of **2f** on the expression of AR-regulated targets*

We showed that compound **2f** is able to reduce AR-transcriptional activity in a dose-dependent manner and to inhibit colony formation of studied PCa cell lines. We further analysed whether **2f** can affect the protein expression of well-known AR transcriptional targets, namely PSA and Nkx3.1 in treated 22Rv1 and C4-2 cells. Immunoblotting analysis (Fig. 9) revealed that protein expression of AR remained unchanged (both full length AR (FL) and V7-splice variant in 22Rv1-ARE14 and predominant full length AR in C4-2), while expression of PSA and Nkx3.1 decreased in dose-dependent manner compared to control, R1881-stimulated cells. This trend is in agreement with luciferase AR-transcriptional assay and is comparable with results observed for galeterone. Moreover, we did not detect the cleaved PARP usually indicating ongoing apoptosis that corresponds with mild cytotoxicity of investigated steroids.

3. Conclusions

A-ring-fused pyrazolo[1,5-*a*]pyrimidine and triazolo[1,5-*a*]pyrimidine derivatives of DHT were efficiently prepared in two steps. Claisen-Schmidt condensation of the steroid precursor with variously substituted aldehydes led to the regio- and stereoselective formation of α,β-unsaturated ketones, which underwent cyclization with 3AT, 3AP and 3AMP, respectively, as binucleophilic reagents. The heterocyclic products were obtained in good yields by spontaneous or induced oxidation.

In addition to the solution phase NMR analysis of the products, the structures of compounds **2a** and **8j** were determined by single crystal X-ray diffraction and both were found to crystallize in the monoclinic crystal system at $P2_1$ space group. In crystal **2a**, the phenyl ring was found to be planar to the DHT part of the molecule. In case of **8j**, the asymmetric unit of the crystal contains two molecules and one CH_2Cl_2 solvent molecule. The thiophene ring is in plane with the DHT rings in one of the molecules, while it turns to almost perpendicular to the DHT ring planes in the second molecule and it occupies two disordered positions. Differences in freedom of rotation can be traced back to secondary interactions with neighbouring molecules.

Our biological experiments revealed us that mainly substituted α,β-enones from series **2** inhibited R1881-stimulated AR transactivation in micromolar concentrations. Candidate compound **2f** showed to interact with the AR in cells and to reduce its transport to the nucleus that resulted in the suppression of expression of AR-regulated proteins observed in androgen-stimulated PCa cell lines. Moreover, we performed a flexible docking study to describe the proposed binding mode of **2f** in the AR-LBD cavity.

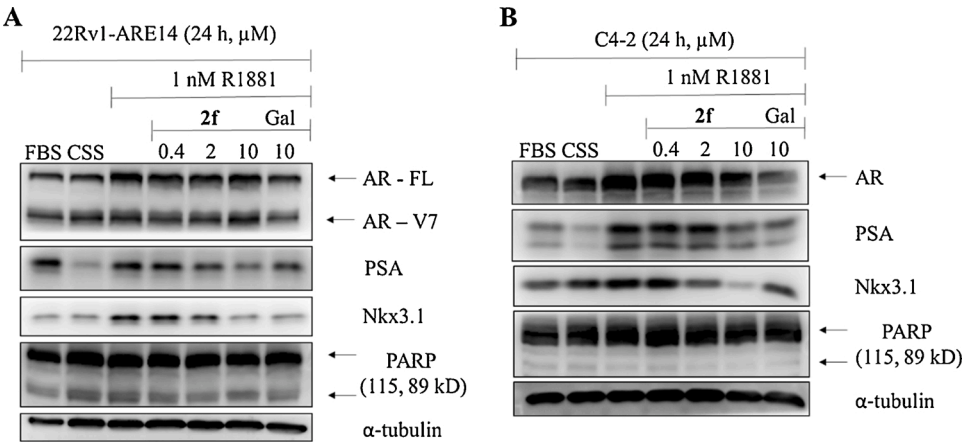

Fig. 9. Western blotting analysis of AR-regulated proteins in treated 22Rv1-ARE14 and C4-2 cell lines. In 22Rv1-ARE14, expression of both full length AR (FL) and V7-splice variant is shown, whereas in C4-2 only predominant full length AR is shown. The cells were deprived of androgens (cultivated in CSS medium) for 24 h and then treated with 1 nM R1881 alone or in combination with different concentrations of **2f** or galeterone for 24 h. Alpha-tubulin was control of equal protein loading. Representative result from two replicates is shown.

4. Experimental

4.1. General

Chemicals, reagents and solvents were purchased from commercial suppliers (Sigma-Aldrich, TCI and Alfa Aesar) and used without further purification. Melting points (Mp) were determined on an SRS Optimelt digital apparatus and are uncorrected. For MW-assisted syntheses, a CEM Discover SP laboratory MW reactor was used with a max. power of 200 W (running a dynamic control program). Elementary analysis data were obtained with a PerkinElmer CHN analyzer model 2400. The transformations were monitored by TLC using 0.25 mm thick Kieselgel-G plates (Si 254 F, Merck). The compound spots were detected by spraying with 5 % phosphomolybdic acid in 50 % aqueous phosphoric acid. Flash chromatographic purifications were carried out on silica gel 60, 40–63 μm (Merck). NMR spectra were recorded with a Bruker DRX 500 instrument at room temperature in $CDCl_3$ using residual solvent signal as an internal reference. Chemical shifts are reported in ppm (δ scale), and coupling constants (J) are given in Hz. Multiplicities of the ^{1}H signals are indicated as a singlet (s), a broad singlet (bs), a doublet (d), a double doublet (dd), a triplet (t), or a multiplet (m). ^{13}C NMR spectra are ^{1}H-decoupled and the J-MOD pulse sequence was used for multiplicity editing. In this spin-echo type experiment, the signal intensity is modulated by the different coupling constants J of carbons depending on the number of attached protons. Both protonated and unprotonated carbons can be detected (CH_3 and CH carbons appear as positive signals, while CH_2 and C carbons as negative signals).

Automated flow injection analyses were performed with an HPLC/MSD system. System accessories: a micro-well plate autoinjector, an Agilent 1100 micro vacuum degasser, a quaternary pump, and a 1946A MSD equipped with an electrospray ion source (ESI) operated in positive ion mode. ESI parameters were: nebulizing gas N_2, at 35 psi; drying gas N_2, at 350 °C and 12 L/min; capillary voltage 3000 V; fragmentor voltage 70 V. The MSD was operated with a mass range of m/z 60 − 620 in scan mode. Samples (0.2 μL) were injected directly into the solvent flow (0.3 mL/min) of acetonitrile/H_2O = 70:30 (v/v) with the simultaneous addition of 0.1 % formic acid with an automated needle wash. Agilent LC/MSD Chemstation was used as software to control the system.

4.2. Chemistry

4.2.1. General procedure for the Claisen-Schmidt condensation of DHT with different (hetero)aryl aldehydes (**1a**–**j**)

DHT (871 mg, 3 mmol) and KOH (281 mg, 5 mmol) were dissolved in absolute EtOH (15 mL) and the mixture was stirred until a homogeneous solution was produced. To this, arylaldehyde (**1a**–j, 3.60 mmol, 1.20 equiv.) was added and the mixture was stirred for a given time at room temperature (**1a**–**e**) or at 0 °C (**1f**–**j**) achieved by an ice bath. After completion of the reaction, the mixture was poured into ice cold water and neutralized with a diluted solution of HCl. The resulting precipitate was filtered off, washed with water, and dried. The crude product was purified by column chromatography (silica gel, CH_2Cl_2 to EtOAc/CH_2Cl_2 = 5:95 using gradient elution).

*4.2.1.1. 17β-Hydroxy-2-benzylidene-5α-androstan-3-one (**2a**).* According to Section *4.2.1.*, benzaldehyde (**1a**, 370 μL) was used for the reaction. The reaction time was 3 h and **2a** was obtained as a white solid. This reaction was repeated several times to obtain a sufficient amount of starting material. Yield: 1.05 g (92 %); Mp 185−187 °C; ^{1}H NMR ($CDCl_3$, 500 MHz): δ 0.73 (s, 3H, 18-H_3), 0.80 (s, 3H, 19-H_3), 0.85–1.02 (overlapping m, 3 H), 1.11 (m, 1 H), 1.22–1.50 (overlapping m, 7 H), 1.58–1.63 (overlapping m, 2 H), 1.71–1.85 (overlapping m, 3 H), 2.07 (m, 1 H), 2.19 (d, 1H, J =15.6 Hz, one of 1-H_2), 2.24 (dd, 1H, J =18.6 Hz, J =13.2 Hz, one of 4-H_2); 2.46 (dd, 1H, J =18.6 Hz, J = 5.2 Hz, the other of 4-H_2), 3.12 (d, 1H, J =15.6 Hz, the other of 1-H_2), 3.65 (t, 1H, J =8.6 Hz, 17-H), 7.33 (m, 1 H), 7.36–7.42 (overlapping m, 4 H), 7.56 (s, 1H, 2a-H); ^{13}C NMR ($CDCl_3$, 125 MHz): δ 11.2 (C-18), 12.0 (C-19), 21.2 (CH_2), 23.5 (CH_2), 28.7 (CH_2), 30.7 (CH_2), 31.2 (CH_2), 35.6 (CH), 36.2 (C-10), 36.8 (CH_2), 42.0 (CH_2), 42.6 (CH), 43.0 (2C, CH_2 and C-13), 51.1 (CH), 53.9 (CH), 82.0 (C-17), 128.5 (2C, C-2′ and C-6′), 128.7 (C-4′), 130.4 (2C, C-3′ and C-5′), 135.4 and 135.8 (C-1′ and C-2) 137.4 (C-2a), 201.6 (C-3); ESI-MS 379 $[M+H]^+$; Anal. Calcd. for $C_{26}H_{34}O_2$ C 82.49; H 9.05. Found C 82.57; H 9.12.

*4.2.1.2. 17β-Hydroxy-2-(4-methyl)benzylidene-5α-androstan-3-one (**2b**).* According to Section *4.2.1.*, *p*-tolualdehyde (**1b**, 420 μL) was used for the reaction. The reaction time was 4 h, and **2b** was obtained as a white solid. Yield: 1.03 g (87 %); Mp 202−205 °C; ^{1}H NMR ($CDCl_3$, 500 MHz): δ 0.73 (s, 3H, 18-H_3), 0.79 (s, 3H, 19-H_3), 0.85–1.02 (overlapping m, 3 H), 1.12 (m, 1 H), 1.21–1.50 (overlapping m, 7 H), 1.58–1.64 (overlapping m, 2 H), 1.70–1.85 (overlapping m, 3 H), 2.07 (m, 1 H), 2.19 (dd, 1H, J =15.7 Hz, J = 2.5 one of 1-H_2), 2.22 (dd, 1H, J =18.6 Hz, J =13.0 Hz, one of 4-H_2), 2.37 (s, 3H, 4′−CH_3), 2.45 (dd, 1H, J =18.6 Hz, J = 5.3 Hz, the other of 4-H_2), 3.11 (d, 1H, J =15.7 Hz, the other of 1-H_2), 3.66 (t, 1H, J =8.6 Hz, 17-H), 7.21 (d, 2H, J =8.1 Hz, 3′-H and 5′-H), 7.30 (d, 2H, J =8.1 Hz, 2′-H and 6′-H), 7.55 (s, 1H, 2a-H); ^{13}C NMR ($CDCl_3$, 125 MHz): δ 11.2 (C-18), 12.0 (C-19), 21.2 (CH_2), 21.5 (4′−CH_3), 23.6 (CH_2), 28.7 (CH_2), 30.7 (CH_2), 31.2 (CH_2), 35.6 (CH), 36.2 (C-10), 36.8 (CH_2), 42.1 (CH_2), 42.6 (CH), 42.9 (CH_2), 43.0 (C-13), 51.1 (CH), 53.9 (CH), 82.0 (C-17), 129.3 (2C, C-2′ and C-6′), 130.6 (2C, C-3′ and C-5′), 133.0 (C-1′), 134.6 (C-4′), 137.6 (C-2a), 139.0 (C-2) 201.6 (C-3); ESI-MS 393 $[M+H]^+$; Anal. Calcd. for $C_{27}H_{36}O_2$ C 82.61; H 9.24. Found C 82.47; H 9.08.

*4.2.1.3. 17β-Hydroxy-2-(3-methyl)benzylidene-5α-androstan-3-one (**2c**).* According to Section *4.2.1.*, *m*-tolualdehyde (**1c**, 420 μL) was used for the reaction. The reaction time was 4 h, and **2c** was obtained as a white solid. Yield: 1.05 g (89 %); Mp 145−147 °C; ^{1}H NMR ($CDCl_3$, 500 MHz): δ 0.73 (s, 3H, 18-H_3), 0.80 (s, 3H, 19-H_3), 0.86–1.02 (overlapping m, 3 H), 1.12 (m, 1 H), 1.22–1.50 (overlapping m, 7 H), 1.58–1.65 (overlapping m, 2 H), 1.71–1.85 (overlapping m, 3 H), 2.07 (m, 1 H), 2.18 (d, 1H, J =15.7 Hz, one of 1-H_2), 2.24 (dd, 1H, J =18.6 Hz, J =13.2 Hz, one of 4-H_2), 2.37 (s, 3H, 3′−CH_3), 2.45 (dd, 1H, J =18.6 Hz, J = 5.3 Hz, the other of 4-H_2), 3.12 (d, 1H, J =15.7 Hz, the other of 1-H_2), 3.65 (t, 1H, J =8.6 Hz, 17-H), 7.14 (d, 1H, J =7.6 Hz, 4′-H), 7.20 (m, 2H, 2′-H and 6′-H), 7.29 (t-like m, 1H, 5′-H), 7.53 (s, 1H, 2a-H); ^{13}C NMR ($CDCl_3$, 125 MHz): δ 11.2 (C-18), 12.0 (C-19), 21.2 (CH_2), 21.6 (3′−CH_3), 23.6 (CH_2), 28.7 (CH_2), 30.7 (CH_2), 31.2 (CH_2), 35.6 (CH), 36.2 (C-10), 36.8 (CH_2), 42.0 (CH_2), 42.7 (CH), 42.9 (CH_2), 43.0 (C-13), 51.1 (CH), 53.9 (CH), 82.0 (C-17), 127.3, 128.4, 129.5 and 131.4 (C-2′, C-4′, C-5′ and C-6′), 135.3 (C-1′), 135.8 (C-2), 137.7 (C-2a), 138.2 (C-3′), 201.6 (C-3); ESI-MS 393 $[M+H]^+$; Anal. Calcd. for $C_{27}H_{36}O_2$ C 82.61; H 9.24. Found C 82.70; H 9.28.

*4.2.1.4. 17β-Hydroxy-2-(4-methoxy)benzylidene-5α-androstan-3-one (**2d**).* According to Section *4.2.1*, *p*-anisaldehyde (**1d**, 440 μL) was used for the reaction. The reaction time was 4 h, and **2d** was obtained as a white solid. Yield: 1.09 g (89 %); Mp 186−188 °C; ^{1}H NMR ($CDCl_3$, 500 MHz): δ 0.74 (s, 3H, 18-H_3), 0.80 (s, 3H, 19-H_3), 0.86–1.02 (overlapping m, 3 H), 1.13 (m, 1 H), 1.20–1.50 (overlapping m, 7 H), 1.58–1.67 (overlapping m, 2 H), 1.71–1.87 (overlapping m, 3 H), 2.07 (m, 1 H), 2.22 (m, 2H, one of 1-H_2 and one of 4-H_2), 2.45 (dd, 1H, J =18.8 Hz, J = 5.3 Hz, the other of 4-H_2), 3.08 (d, 1H, J =15.7 Hz, the other of 1-H_2), 3.66 (t, 1H, J =8.6 Hz, 17-H), 3.84 (s, 3H, 4′−OCH_3), 6.93 (d, 2H, J =8.8 Hz, 3′-H and 5′-H), 7.38 (d, 2H, J =8.8 Hz, 2′-H and 6′-H), 7.55 (s, 1H, 2a-H); ^{13}C NMR ($CDCl_3$, 125 MHz): δ 11.2 (C-18), 12.1 (C-19), 21.2 (CH_2), 23.6 (CH_2), 28.7 (CH_2), 30.7 (CH_2), 31.2 (CH_2), 35.6 (CH), 36.1 (C-10), 36.9 (CH_2), 42.2 (CH_2), 42.4 (CH), 42.8 (CH_2), 43.0 (C-13), 51.1 (CH), 54.0 (CH), 55.5 (4′−OCH_3), 82.0 (C-17), 114.1 (2C, C-3′ and C-5′), 128.4 (C-1′), 132.4 (2C, C-2′ and C-6′), 133.3 (C-2), 137.6 (C-2a), 160.1 (C-4′) 201.4 (C-3); ESI-MS 409 $[M+H]^+$; Anal. Calcd. for $C_{27}H_{36}O_3$ C 79.37; H 8.88. Found C 79.25; H 9.01.

*4.2.1.5. 17β-Hydroxy-2-(4-fluoro)benzylidene-5α-androstan-3-one (**2e**).* According to Section *4.2.1.*, 4-fluorobenzaldehyde (**1e**, 390 μL) was used for the reaction. The reaction time was 3 h, and **2e** was obtained as a white solid. Yield: 1.08 g (91 %); Mp 107−111 °C; ^{1}H NMR ($CDCl_3$, 500 MHz): δ 0.74 (s, 3H, 18-H_3), 0.81 (s, 3H, 19-H_3), 0.85–1.02 (overlapping m, 3 H), 1.12 (m, 1 H), 1.22–1.51 (overlapping m, 7 H), 1.57–1.65 (overlapping m, 2 H), 1.72–1.86 (overlapping m, 3 H), 2.07 (m, 1 H), 2.17 (d, 1H, J =15.7 Hz, one of 1-H_2), 2.24 (dd, 1H, J =18.6 Hz, J =13.2 Hz, one of 4-H_2), 2.45 (dd, 1H, J =18.6 Hz, J = 5.3 Hz, the other of 4-H_2), 3.05 (d, 1H, J =15.7 Hz, the other of 1-H_2), 3.66 (t, 1H, J =8.6 Hz, 17-H), 7.09 (m, 2H, J =8.1 Hz, 3′-H and 5′-H), 7.36 (m, 2H, 2′-H and 6′-H), 7.51 (s, 1H, 2a-H); ^{13}C NMR ($CDCl_3$, 125 MHz): δ 11.2 (C-18), 12.1 (C-19), 21.2 (CH_2), 23.6 (CH_2), 28.7 (CH_2), 30.8 (CH_2), 31.3 (CH_2), 35.7 (CH), 36.3 (C-10), 36.9 (CH_2), 42.0 (CH_2), 42.7 (CH), 42.9 (CH_2), 43.1 (C-13), 51.2 (CH), 54.0 (CH), 82.0 (C-17), 115.7 (d, 2C, J =21.5 Hz, C-3′ and C-5′), 132.0 (C-1′), 132.3 (d, 2C, J =8.3 Hz, C-2′ and C-6′), 135.3 (C-2), 136.2 (C-2a), 161.8 (d, J =250.0 Hz, C-4′), 201.3 (C-3); ESI-MS 397 $[M+H]^+$; Anal. Calcd. for $C_{26}H_{33}FO_2$ C 78.75; H 8.39. Found C 78.84; H 8.29.

*4.2.1.6. 17β-Hydroxy-2-(4-chloro)benzylidene-5α-androstan-3-one (**2f**).* According to Section *4.2.1.*, 4-chlorobenzaldehyde (**1f**, 506 mg) was used for the reaction. The reaction time was 3 h, and **2f** was obtained as a white solid. Yield: 1.12 g (90 %); Mp 195−197 °C; ^{1}H NMR ($CDCl_3$, 500 MHz): δ 0.73 (s, 3H, 18-H_3), 0.80 (s, 3H, 19-H_3), 0.85–1.01 (overlapping m, 3 H), 1.11 (m, 1 H), 1.22–1.50 (overlapping m, 7 H), 1.56–1.65 (overlapping m, 2 H), 1.72–1.86 (overlapping m, 3 H), 2.06 (m, 1 H), 2.22 (d, 1H, J =15.7 Hz, one of 1-H_2), 2.22 (dd, 1H, J =18.7 Hz, J =13.3 Hz, one of 4-H_2), 2.45 (dd, 1H, J =18.7 Hz, J = 5.3 Hz, the other of 4-H_2), 3.03 (d, 1H, J =15.7 Hz, the other of 1-H_2), 3.65 (t, 1H, J =8.6 Hz, 17-H), 7.30 (d, 2H, J =8.6 Hz, 3′-H and 5′-H), 7.37 (d, 2H, J =8.6 Hz, 2′-H and 6′-H), 7.48 (s, 1H, 2a-H); ^{13}C NMR ($CDCl_3$, 125 MHz): δ 11.2 (C-18), 12.0 (C-19), 21.2 (CH_2), 23.5 (CH_2), 28.7 (CH_2), 30.7 (CH_2), 31.2 (CH_2), 35.6 (CH), 36.3 (C-10), 36.8 (CH_2), 42.0 (CH_2), 42.6 (CH), 42.9 (CH_2), 43.0 (C-13), 51.1 (CH), 53.9 (CH), 82.0 (C-17), 128.8 (2C, C-3′ and C-5′), 131.6 (2C, C-2′ and C-6′), 134.2 (C-4′), 134.6 (C-1′), 136.0 (C-2), 136.0 (C-2a), 201.4 (C-3); ESI-MS 413 $[M+H]^+$; Anal. Calcd. for $C_{26}H_{33}ClO_2$ C 75.61; H 8.05. Found C 75.49; H 7.92.

*4.2.1.7. 17β-Hydroxy-2-(2-furylidene)-5α-androstan-3-one (**2i**).* According to Section *4.2.1.*, furfural (**1i**, 300 μL) was used for the reaction. The reaction time was 3 h, and **2i** was obtained as a pale yellow solid. Yield: 926 mg (84 %); Mp 197−199 °C; ^{1}H NMR ($CDCl_3$, 500 MHz): δ 0.77 (s, 3H, 18-H_3), 0.86 (s, 3H, 19-H_3), 0.88–1.04 (overlapping m, 3 H), 1.16 (m, 1 H), 1.22–1.33 (overlapping m, 2 H), 1.37–1.50 (overlapping m, 4 H), 1.62 (m, 1 H), 1.72–1.80 (overlapping m, 3 H), 1.90 (m, 1 H), 2.08 (m, 1 H), 2.18 (d, 1H, J =17.5 Hz, one of 1-H_2), 2.22 (dd, 1H, J =19.0 Hz, J =13.2 Hz, one of 4-H_2), 2.41 (dd, 1H, J =19.0 Hz, J = 5.4 Hz, the other of 4-H_2), 3.25 (d, 1H, J =17.5 Hz, the other of 1-H_2), 3.67 (t, 1H, J =8.6 Hz, 17-H), 6.51 (dd, 1H, J =3.4 Hz, J =1.8 Hz, 4′-H), 6.62 (d, 1H, J =3.4 Hz, 3′-H), 7.40 (d, 1H, J =1.8 Hz, 5′-H), 7.57 (s, 1H, 2a-H); ^{13}C NMR ($CDCl_3$, 125 MHz): δ 11.2 (C-18), 12.4 (C-19), 21.3 (CH_2), 23.6 (CH_2), 28.7 (CH_2), 30.8 (CH_2), 31.3 (CH_2), 35.6 (C-10), 35.7 (CH), 37.0 (CH_2), 42.1 (CH), 42.2 (CH_2), 42.5 (CH_2), 43.1 (C-13), 51.2 (CH), 54.1 (CH), 82.1 (C-17), 112.4 (C-3′), 116.3 (C-4′), 124.3 (C-2a), 131.9 (C-2), 144.8 (C-5′), 152.6 (C-2′), 200.3 (C-3); ESI-MS 369 $[M+H]^+$; Anal. Calcd. for $C_{24}H_{32}O_3$ C 78.22; H 8.75. Found C 78.11; H 8.82.

*4.2.1.8. 17β-Hydroxy-2-(2-thiophenylidene)-5α-androstan-3-one (**2j**).* According to Section *4.2.1.*, thiophene-2-carbaldehyde (**1j**, 340 μL) was used for the reaction. The reaction time was 3 h, and **2j** was obtained as a pale yellow solid. Yield: 962 mg (83 %); Mp 216−219 °C; ^{1}H NMR ($CDCl_3$, 500 MHz): δ 0.77 (s, 3H, 18-H_3), 0.86 (s, 3H, 19-H_3), 0.90–1.04 (overlapping m, 3 H), 1.18 (m, 1 H), 1.23–1.33 (overlapping m, 2 H), 1.37–1.53 (overlapping m, 4 H), 1.63 (m, 1 H), 1.72–1.82 (overlapping m, 3 H), 1.91 (m, 1 H), 2.08 (m, 1 H), 2.18 (d, 1H, J =16.5 Hz, one of 1-H_2), 2.24 (dd, 1H, J =19.1 Hz, J =13.1 Hz, one of 4-H_2), 2.43 (dd, 1H, J =19.1 Hz, J = 5.4 Hz, the other of 4-H_2), 3.11 (d, 1H, J =16.5 Hz, the other of 1-H_2), 3.68 (t, 1H, J =8.6 Hz, 17-H), 7.14 (dd, 1H, J = 5.1 Hz, J =3.7 Hz, 4′-H), 7.35 (d, 1H, J =3.7 Hz, 3′-H), 7.54 (d, 1H, J = 5.1 Hz, 5′-H), 7.84 (s, 1H, 2a-H); ^{13}C NMR ($CDCl_3$, 125 MHz): δ 11.2 (C-18), 12.5 (C-19), 21.3 (CH_2), 23.6 (CH_2), 28.7 (CH_2), 30.7 (CH_2), 31.2 (CH_2), 35.6 (CH), 35.9 (C-10), 36.9 (CH_2), 41.8 (CH), 42.4 (CH_2), 42.6 (CH_2), 43.1 (C-13), 51.1 (CH), 54.0 (CH), 82.0 (C-17), 127.8 (C-4′), 130.3 (C-2a), 130.7 (C-3′), 131.5 (C-2′), 133.6 (C-5′), 139.3 (C-2), 200.3 (C-3); ESI-MS 385 $[M+H]^+$; Anal. Calcd. for $C_{24}H_{32}O_2S$ C 74.96; H 8.39. Found C 74.84; H 8.27.

*4.2.2. General procedure for the synthesis of A-ring-fused pyrazolo[1,5-a] pyrimidine (**6a, 7a**) and triazolo[1,5-a]pyrimidine derivatives (**8a**−**f**, **8i**−**k**) of DHT*

1 mmol arylidene (**2a**−**f**), heteroarylidene (**2i**, **2 j**) or methylidene derivative (**2k**) [21], binucleophil reagent (3-amino-5-methylpyrazole - 3AMP, 3-aminopyrazole - 3AP or 3-aminotriazole - 3AT, 2 equiv.) and *t*-BuOK (224 mg, 2 equiv.) were dissolved in DMF (10 mL) and the mixture was stirred at 140 °C for 45 min. After complete conversion of the starting material, the mixture was stirred for another 24 h at room temperature, while spontaneous oxidation of the heteroring occurred in most of the cases. During work-up, the mixture was poured into water, neutralized with diluted HCl and extracted with CH_2Cl_2 (3 × 10 mL). The combined organic layer was washed with water (2 × 20 mL) and

brine (20 mL), dried over anhydrous Na_2SO_4 and the solvent was evaporated *in vacuo*. The crude product was purified by column chromatography except in the reaction of **2f** with 3AT, where oxidation of the heteroring with DDQ was needed. Thus, in this latter case, the residue was dissolved in 1,4-dioxane (10 mL) and DDQ (499 mg, 1.1 equiv.) was added. The mixture was irradiated in a closed vessel at 120 °C for 5 min, then poured into ice-cold water. NH_4Cl was added and the resulting precipitate was filtered off and dried. The crude product was purified by column chromatography.

*4.2.2.1. 17β-Hydroxy-2′-methyl-7′-phenylpyrazolo[1,5-a]pyrimidino [5′,6′-3,2]-5α-androstane (**6a**).* Substrate: **2a** (379 mg); Reagent: 3AMP (194 mg). For purification of the crude product, EtOAc/CH_2Cl_2 = 20:80 eluent was used. Yield: 237 mg (52 %, off white solid); Mp 259−261 °C; ^{1}H NMR ($CDCl_3$, 500 MHz): δ 0.71 (s, 3H, 18-H_3), 0.74 (s, 3H, 19-H_3), 0.86–1.04 (overlapping m, 4 H), 1.23–1.45 (overlapping m, 6 H), 1.58–1.76 (overlapping m, 5 H), 2.05 (m, 1 H), 2.18 (d, 1H, J =16.0 Hz, 1α -H), 2.41 (s, 3H, 2′−CH_3), 2.56 (d, 1H, J =16.0 Hz, 1β-H), 2.72 (dd, 1H, J =18.9 Hz, J =12.6 Hz, 4β-H), 3.03 (dd, 1H, J =18.9 Hz, J = 5.6 Hz, 4α-H), 3.61 (t, 1H, J =8.6 Hz, 17α-H), 6.40 (d, 1H, J =2.4 Hz, 3′-H), 7.44 (bs, 2H, 2″-H and 6″-H), 7.53–7.59 (m, 3H, 3″-H, 4″-H and 5″-H); ^{13}C NMR ($CDCl_3$, 125 MHz): δ 11.1 (C-18), 11.7 (C-19), 14.9 (2′−CH_3), 20.8 (C-11), 23.4 (C-15), 28.5 (C-6), 30.5 (C-16), 31.1 (C-7), 35.3 (C-10), 35.6 (C-8), 36.6 (C-4), 37.1 (C-12), 40.0 (C-1), 41.6 (C-5), 42.8 (C-13), 50.9 (C-14), 53.5 (C-9), 81.8 (C-17), 94.1 (C-3′), 114.1 (C-2), 128.9 (2C) and 129.3 (2C): C-2″, C-6″, C-3″ and C-5″, 129.9 (C-4″), 130.5 (C-4″), 144.4 (C), 148.3 (C), 154.6 (C), 158.4 (C-3); ESI-MS 456 $[M+H]^+$; Anal. Calcd. for $C_{30}H_{37}N_3O$ C 79.08; H 8.19. Found C 79.01; H 8.07.

*4.2.2.2. In the PDF, section 4.2.2.2. and 4.2.2.5. are next to each other, but the text seems completely different (this is just an example). Could the line spacing and editing be unified? 17β-Hydroxy-7′-phenylpyrazolo[1,5-a] pyrimidino[5′,6′-3,2]-5α-androstane (**7a**).* Substrate: **2a** (379 mg); Reagent: 3AP (166 mg). For purification of the crude product, EtOAc/CH_2Cl_2 = 20:80 eluent was used. Yield: 270 mg (61 %, yellow solid); Mp 140−142 °C; ^{1}H NMR ($CDCl_3$, 500 MHz): δ 0.72 (s, 3H, 18-H_3), 0.78 (s, 3H, 19-H_3), 0.80 (m, 1H, 9α-H), 0.92−0.99 (overlapping m, 2H, 7α-H and 14α-H), 1.02 (m, 1H, 12α-H), 1.23–1.47 (overlapping m, 6H, 15β-H, 11-H_2, 6β-H, 8β-H and 16β-H), 1.58–1.79 (overlapping m, 5H, 5α-H, 6α-H, 7β-H, 12β-H and 15α-H), 2.06 (m, 1H, 16α-H), 2.23 (d, 1H, J =16.2 Hz, 1α -H), 2.65 (d, 1H, J =16.2 Hz, 1β-H), 2.76 (dd, 1H, J =19.2 Hz, J =12.7 Hz, 4β-H), 3.09 (dd, 1H, J =19.2 Hz, J = 5.6 Hz, 4α-H), 3.62 (t, 1H, J =8.6 Hz, 17α-H), 6.63 (d, 1H, J =2.4 Hz, 3′-H), 7.45 (bd, 2H, 2″-H and 6″-H), 7.54–7.61 (m, 3H, 3″-H, 4″-H and 5″-H), 7.99 (d, 1H, J =2.4 Hz, 2′-H); ^{13}C NMR ($CDCl_3$, 125 MHz): δ 11.2 (C-18), 11.8 (C-19), 20.9 (C-11), 23.6 (C-15), 28.6 (C-6), 30.8 (C-16), 31.2 (C-7), 35.5 (C-10), 35.8 (C-8), 36.8 (2C: C-4 and C-12), 40.1 (C-1), 41.8 (C-5), 43.0 (C-13), 51.2 (C-14), 53.8 (C-9), 82.0 (C-17), 94.8 (C-3′), 115.2 (C-2), 129.2 (2C) and 129.3 (2C): C-2″, C-6″, C-3″ and C-5″), 130.3 (C-1″), 130.4 (C-4″), 144.9 (C-2′), 145.8 and 146.9 (C-3a’ and C-7′), 159.0 (C-3); ESI-MS 442 $[M+H]^+$; Anal. Calcd. for $C_{29}H_{35}N_3O$ C 78.87; H 7.99. Found C 79.01; H 8.07.

*4.2.2.3. 17β-Hydroxy-7′-phenyl[1,2,4]triazolo[1,5-a]pyrimidino [5′,6′:3,2]-5α-androstane (**8a**).* Substrate: **2a** (379 mg); Reagent: 3AT (168 mg). For purification of the crude product, EtOAc/CH_2Cl_2 = 50:50 eluent was used. Yield: 317 mg (72 %, white solid); Mp 257−260 °C; ^{1}H NMR ($CDCl_3$, 500 MHz): δ 0.71 (s, 3H, 18-H_3), 0.75 (s, 3H, 19-H_3), 0.82 (m, 1H, 9α-H), 0.90–1.06 (overlapping m, 3H, 7α-H, 12α-H and 14α-H), 1.22–1.46 (overlapping m, 6H, 6β-H, 8β-H, 11-H_2, 15β-H and 16β-H), 1.57–1.77 (overlapping m, 5H, 5α-H, 6α-H, 7β-H, 12β-H and 15α-H), 2.05 (m, 1H, 16α-H), 2.32 (d, 1H, J =16.2 Hz, 1α-H), 2.71 (d, 1H, J =16.2 Hz, 1β-H), 2.81 (dd, 1H, J =19.4 Hz, J =12.8 Hz, 4β-H), 3.13 (dd, 1H, J =19.4 Hz, J = 5.3 Hz, 4α-H), 3.62 (t, 1H, J =8.5 Hz, 17α-H), 7.48 (m, 2H, 2″-H and 6″-H), 7.60 (m, 3H, 3″-H, 4″-H and 5″-H), 8.33 (s, 1H, 2′-H); ^{13}C NMR ($CDCl_3$, 125 MHz): δ 11.1 (C-18), 11.8 (C-19), 20.9 (C-11), 23.5 (C-15), 28.3 (C-6), 30.6 (C-16), 31.1 (C-7), 35.3 (C-10), 35.6 (C-8), 36.6 (C-12), 37.6 (C-4), 40.0 (C-1), 41.5 (C-5), 42.9 (C-13), 50.9 (C-14), 53.5 (C-9), 81.9 (C-17), 118.1 (C-2), 129.1 (C-1″), 129.2 (4C, C-2″, C-3″, C-5″ and C-6″), 130.9 (C-4″), 146.0 (C-7′), 153.7 (C-3a’), 155.1 (C-2′), 165.9 (C-3); ESI-MS 443 $[M+H]^+$; Anal. Calcd. for $C_{28}H_{34}N_4O$ C 75.98; H 7.74. Found C 76.12; H 7.66.

*4.2.2.4. 17β-Hydroxy-7′-(4″-tolyl)-[1,2,4]triazolo[1,5-a]pyrimidino [5′,6′:3,2]-5α-androstane (**8b**).* Substrate: **2b** (393 mg); Reagent: 3AT (168 mg). For purification of the crude product, EtOAc/CH_2Cl_2 = 40:60 eluent was used. Yield: 349 mg (76 %, white solid); Mp 135−138 °C; ^{1}H NMR ($CDCl_3$, 500 MHz): δ 0.72 (s, 3H, 18-H_3), 0.76 (s, 3H, 19-H_3), 0.83 (m, 1 H), 0.92–1.08 (overlapping m, 3 H), 1.26–1.47 (overlapping m, 6 H), 1.59–1.79 (overlapping m, 5 H), 2.07 (m, 1 H), 2.35 (d, 1H, J =16.3 Hz, 1α-H), 249 (s, 3H, 4″−CH_3), 2.78 (d, 1H, J =16.3 Hz, 1β-H), 2.83 (dd, 1H, J =19.6 Hz, J =13.0 Hz, 4β-H), 3.15 (dd, 1H, J =19.6 Hz, J = 5.3 Hz, 4α-H), 3.63 (t, 1H, J =8.6 Hz, 17α-H), 7.41 (m, 4H, 2″-H, 3″-H, 5″-H and 6″-H), 8.39 (s, 1H, 2′-H); ^{13}C NMR ($CDCl_3$, 125 MHz): δ 11.2 (C-18), 11.8 (C-19), 21.0 (C-11), 21.8 (4″−CH_3), 23.5 (C-15), 28.4 (C-6), 30.7 (C-16), 31.1 (C-7), 35.4 (C-10), 35.7 (C-8), 36.7 (C-12), 37.8 (C-4), 40.2 (C-1), 41.5 (C-5), 42.9 (C-13), 51.0 (C-14), 53.6 (C-9), 82.0 (C-17), 118.8 (C-2), 125.7 (C-1″), 129.2 (2C, C-2″ and C-6″), 129.9 (2C, C-3″ and C-5″), 141.5 (C-4″), 146.6 (C-7′), 166.9 (C-3); the signals for C-2′ and C-3a’ were not observed; ESI-MS 457 $[M+H]^+$; Anal. Calcd. for $C_{29}H_{36}N_4O$ C 76.28; H 7.95. Found C 76.35; H 8.07.

*4.2.2.5. 17β-Hydroxy-7′-(3″-tolyl)-[1,2,4]triazolo[1,5-a]pyrimidino [5′,6′:3,2]-5α-androstane (**8c**).* Substrate: **2c** (393 mg); Reagent: 3AT (168 mg). For purification of the crude product, EtOAc/CH_2Cl_2 = 40:60 eluent was used. Yield: 351 mg (77 %, white solid); Mp 160−163 °C; ^{1}H NMR ($CDCl_3$, 500 MHz): δ 0.72 (s, 3H, 18-H_3), 0.77 (s, 3H, 19-H_3), 0.81–1.07 (overlapping m, 4 H), 9α-H), 1.24–1.47 (overlapping m, 6 H), 1.59–1.89 (overlapping m, 5 H), 2.06 (m, 1 H), 2.30 (d, 1H, J =16.3 Hz, 1α-H), 247 (s, 3H, 3″−CH_3), 2.71 (d, 1H, J =16.3 Hz, 1β-H), 2.81 (dd, 1H, J =19.5 Hz, J =12.7 Hz, 4β-H), 3.14 (dd, 1H, J =19.5 Hz, J = 5.6 Hz, 4α-H), 3.63 (t, 1H, J =8.6 Hz, 17α-H), 7.25 (m, 2 H), 7.40 (d-like m, 1 H): 2″-H, 4″-H and 6″-H, 7.49 (t-like m, 1H, 5″-H), 8.34 (s, 1H, 2′-H); ^{13}C NMR ($CDCl_3$, 125 MHz): δ 11.2 (C-18), 11.8 (C-19), 20.9 (C-11), 21.7 (3″−CH_3), 23.5 (C-15), 28.4 (C-6), 30.7 (C-16), 31.1 (C-7), 35.3 (C-10), 35.7 (C-8), 36.7 (C-12), 37.7 (C-4), 40.1 (C-1), 41.6 (C-5), 42.9 (C-13), 51.0 (C-14), 53.6 (C-9), 82.0 (C-17), 118.1 (C-2), 126.2 (C-6″), 129.1 (C-1″), 129.2, 129.5 and 131.7 (C-2″, C-4″ and C-5″), 139.1 (C-4″), 146.4 (C-7′), 153.8 (C-3a’), 155.2 (C-2′), 165.8 (C-3); ESI-MS 457 $[M+H]^+$; Anal. Calcd. for $C_{29}H_{36}N_4O$ C 76.28; H 7.95. Found C 76.15; H 7.88.

*4.2.2.6. 17β-Hydroxy-7′-(4″-methoxyphenyl)-[1,2,4]triazolo[1,5-a]pyrimidino[5′,6′:3,2]-5α-androstane (**8d**).* Substrate: **2d** (409 mg); Reagent: 3AT (168 mg). For purification of the crude product, EtOAc/CH_2Cl_2 = 40:60 eluent was used. Yield: 337 mg (71 %, off white solid); Mp 158−161 °C; ^{1}H NMR ($CDCl_3$, 500 MHz): δ 0.73 (s, 3H, 18-H_3), 0.75 (s, 3H, 19-H_3), 0.82 (m, 1 H), 0.92–1.09 (overlapping m, 3 H), 1.26–1.47 (overlapping m, 6 H), 1.59–1.80 (overlapping m, 5 H), 2.07 (m, 1 H), 2.35 (d, 1H, J =16.3 Hz, 1α-H), 2.77 (d, 1H, J =16.3 Hz, 1β-H), 2.82 (dd, 1H, J =19.6 Hz, J =13.0 Hz, 4β-H), 3.15 (dd, 1H, J =19.6 Hz, J = 5.3 Hz, 4α-H), 3.64 (t, 1H, J =8.6 Hz, 17α-H), 3.91 (s, 3H, 4″- OMe), 7.11 (d, 2H, J =8.8 Hz, 3″-H and 5″-H), 7.47 (d, 2H, J =8.8 Hz, 2″-H and 6″-H), 8.36 (s, 1H, 2′-H); ^{13}C NMR ($CDCl_3$, 125 MHz): δ 11.2 (C-18), 11.8 (C-19), 21.0 (C-11), 23.6 (C-15), 28.4 (C-6), 30.8 (C-16), 31.2 (C-7), 35.4 (C-10), 35.8 (C-8), 36.8 (C-12), 37.8 (C-4), 40.4 (C-1), 41.7 (C-5), 43.0 (C-13), 51.1 (C-14), 53.7 (C-9), 55.6 (4″- OMe), 82.0 (C-17), 114.6 (2C, C-3″ and C-5″), 118.4 (C-2), 120.9 (C-1″), 131.2 (2C, C-2″ and C-6″), 146.2 (C-7′), 153.3 (C-3a’), 154.4 (C-2′), 161.5 (C-4″), 166.3 (C-3); ESI-MS 473 $[M+H]^+$; Anal. Calcd. for $C_{29}H_{36}N_4O_2$ C 73.70; H 7.68. Found C 73.82; H 7.57.

*4.2.2.7. 17β-Hydroxy-7′-(4″-fluorophenyl)-[1,2,4]triazolo[1,5-a]pyrimidino[5′,6′:3,2]-5α-androstane (**8e**).* Substrate: **2e** (397 mg); Reagent: 3AT (168 mg). For purification of the crude product, EtOAc/CH_2Cl_2 = 50:50 eluent was used. Yield: 335 mg (73 %, off white solid); Mp 135−138 °C; ^{1}H NMR ($CDCl_3$, 500 MHz): δ 0.73 (s, 3H, 18-H_3), 0.76 (s, 3H, 19-H_3), 0.80–1.08 (overlapping m, 4 H), 1.25–1.48 (overlapping m, 6 H), 1.59–1.81 (overlapping m, 5 H), 2.07 (m, 1 H), 2.32 (d, 1H, *J* =16.2 Hz, 1α-H), 2.70 (d, 1H, *J* =16.2 Hz, 1β-H), 2.81 (dd, 1H, *J* =19.5 Hz, *J* =12.7 Hz, 4β-H), 3.15 (dd, 1H, *J* =19.5 Hz, *J* = 5.6 Hz, 4α-H), 3.63 (t, 1H, *J* =8.6 Hz, 17α-H), 7.31 (m, 2H, 3″-H and 5″-H), 7.51 (m, 2H, 2″-H and 6″-H), 8.34 (s, 1H, 2′-H); ^{13}C NMR ($CDCl_3$, 125 MHz): δ 11.2 (C-18), 11.8 (C-19), 21.0 (C-11), 23.5 (C-15), 28.4 (C-6), 30.7 (C-16), 31.1 (C-7), 35.4 (C-10), 35.7 (C-8), 36.7 (C-12), 37.7 (C-4), 40.2 (C-1), 41.6 (C-5), 42.9 (C-13), 51.0 (C-14), 53.6 (C-9), 82.0 (C-17), 116.6 (d, 2C, *J* =22.1 Hz, C-3″ and C-5″), 118.1 (C-2), 125.1 (d, *J* =3.5 Hz, C-1″), 131.7 (d, 2C, *J* =8.6 Hz, C-2″ and C-6″), 145.0 (C-7′), 154.0 (C-3a'), 155.4 (C-2′), 164.0 (d, *J* =252.1 Hz, C-4″), 165.8 (C-3); ESI-MS 461 $[M+H]^+$; Anal. Calcd. for $C_{28}H_{33}FN_4O$ C 73.02; H 7.22. Found C 72.95; H 7.13.

*4.2.2.8. 17β-Hydroxy-7′-(4″-chlorophenyl)-[1,2,4]triazolo[1,5-a]pyrimidino[5′,6′:3,2]-5α-androstane (**8f**).* Substrate: **2f** (413 mg); Reagent: 3AT (168 mg). For purification of the crude product after oxidation with DDQ, EtOAc/CH_2Cl_2 = 50:50 eluent was used. Yield: 311 mg (65 %, white solid); Mp 157−160 °C; ^{1}H NMR ($CDCl_3$, 500 MHz): δ 0.73 (s, 3H, 18-H_3), 0.76 (s, 3H, 19-H_3), 0.84 (m, 1 H), 0.92–1.09 (overlapping m, 3 H), 1.24–1.48 (overlapping m, 6 H), 1.60–1.81 (overlapping m, 5 H), 2.07 (m, 1 H), 2.32 (d, 1H, *J* =16.2 Hz, 1α-H), 2.71 (d, 1H, *J* =16.2 Hz, 1β-H), 2.82 (dd, 1H, *J* =19.7 Hz, *J* =12.8 Hz, 4β-H), 3.15 (dd, 1H, *J* =19.7 Hz, *J* = 5.3 Hz, 4α-H), 3.64 (t, 1H, *J* =8.6 Hz, 17α-H), 7.45 (d, 2H, *J* =8.2 Hz, 3″-H and 5″-H), 7.60 (d, 2H, *J* =8.2 Hz, 2″-H and 6″-H), 8.33 (s, 1H, 2′-H); ^{13}C NMR ($CDCl_3$, 125 MHz): δ 11.2 (C-18), 11.9 (C-19), 21.1 (C-11), 23.6 (C-15), 28.5 (C-6), 30.8 (C-16), 31.2 (C-7), 35.5 (C-10), 35.8 (C-8), 36.8 (C-12), 37.7 (C-4), 40.2 (C-1), 41.7 (C-5), 43.0 (C-13), 51.1 (C-14), 53.7 (C-9), 82.0 (C-17), 118.0 (C-2), 127.6 (C-1″), 129.6 (2C, C-2″ and C-6″), 130.9 (2C, C-3″ and C-5″), 137.2 (C-4″), 144.8 (C-7′), 154.1 (C-3a'), 155.6 (C-2′), 165.7 (C-3); ESI-MS 477 $[M+H]^+$; Anal. Calcd. for $C_{28}H_{33}ClN_4O$ C 70.50; H 6.97. Found C 70.69; H 7.07.

*4.2.2.9. 17β-Hydroxy-7′-(furan-2″-yl)-[1,2,4]triazolo[1,5-a]pyrimidino[5′,6′:3,2]-5α-androstane (**8i**).* Substrate: **2i** (369 mg); Reagent: 3AT (168 mg). For purification of the crude product, EtOAc/CH_2Cl_2 = 40:60 eluent was used. ; ^{1}H NMR ($CDCl_3$, 500 MHz): δ 0.78 (s, 3H, 18-H_3), 0.79 (s, 3H, 19-H_3, 0.94–1.06 (overlapping m, 3 H), 1.16–1.53 (overlapping m, 6 H), 1.62–1.81 (overlapping m, 5 H), 1.90 (m, 1 H), 2.10 (m, 1 H), 2.75 (d, 1H, *J* =17.1 Hz, 1α -H), 2.84 (dd, 1H, *J* =19.4 Hz, *J* =12.7 Hz, 4β-H), 3.11 (dd, 1H, *J* =19.4 Hz, *J* = 5.5 Hz, 4α-H), 3.36 (d, 1H, *J* =17.1 Hz, 1β -H), 3.69 (t, 1H, *J* =8.6 Hz, 17α-H), 6.78 (dd, 1H, *J* =3.6 Hz, *J* =1.7 Hz, 4″-H), 7.83 (d, 1H, *J* =1.7 Hz, 3″-H), 8.10 (d, 1H, *J* =3.6 Hz, 5″-H), 8.48 (s, 1H, 2′-H); ^{13}C NMR ($CDCl_3$, 125 MHz): δ 11.2 (C-18), 12.0 (C-19), 21.2 (C-11), 23.6 (C-15), 28.3 (C-6), 30.8 (C-16), 31.2 (C-7), 35.0 (C-10), 35.7 (C-8), 36.9 (C-12), 37.9 (C-4), 40.7 (C-1), 40.9 (C-5), 43.0 (C-13), 51.1 (C-14), 54.0 (C-9), 82.0 (C-17), 112.6 (C-3″), 117.1 (C-2), 121.8 (C-4″), 135.4 (C-2″), 143.9 (C-7′), 146.0 (C-5″), 153.4 (C-3a'), 154.5 (C-2′), 165.7 (C-3); ESI-MS 433 $[M+H]^+$; Anal. Calcd. for $C_{26}H_{32}N_4O_2$ C 72.19; H 7.46. Found C 72.27; H 7.33.

*4.2.2.10. 17β-Hydroxy-7′-(thiophen-2″-yl)-[1,2,4]triazolo[1,5-a]pyrimidino[5′,6′:3,2]-5α-androstane (**8j**).* Substrate: **2j** (385 mg); Reagent: 3AT (168 mg). For purification of the crude product, EtOAc/CH_2Cl_2 = 40:60 eluent was used. Yield: 280 mg (62 %, yellow solid); Mp 164−167 °C; ^{1}H NMR ($CDCl_3$, 500 MHz): δ 0.75 (s, 3H, 18-H_3), 0.76 (s, 3H, 19-H_3), 0.89–1.04 (overlapping m, 3 H), 1.13 (m, 1 H), 1.25–1.49 (overlapping m, 5 H), 1.54–1.87 (overlapping m, 6 H), 2.08 (m, 1 H), 2.53 (d, 1H, *J* =16.2 Hz, 1α-H), 2.83 (dd, 1H, *J* =19.6 Hz, *J* =12.7 Hz, 4β-H), 3.08 (d, 1H, *J* =16.2 Hz, 1β -H), 3.16 (dd, 1H, *J* =19.6 Hz, *J* = 5.7 Hz, 4α-H), 3.66 (t, 1H, *J* =8.6 Hz, 17α-H), 7.32 (dd, 1H, *J* = 5.0 Hz, *J* =3.8 Hz, 4″-H), 7.80 (m, 2H, 3″-H and 5″-H), 8.46 (s, 1H, 2′-H); ^{13}C NMR ($CDCl_3$, 125 MHz): δ 11.2 (C-18), 11.9 (C-19), 21.2 (C-11), 23.5 (C-15), 28.3 (C-6), 30.7 (C-16), 31.1 (C-7), 35.6 (C-10), 35.7 (C-8), 36.8 (C-12), 37.8 (C-4), 41.3 (C-5), 41.4 (C-1), 43.0 (C-13), 51.0 (C-14), 53.8 (C-9), 82.0 (C-17), 118.8 (C-2), 127.4 (C-3″), 128.1 (C-2″), 131.4 (C-4″), 133.9 (C-5″), 140.4 (C-7′), 153.0 (C-3a'), 153.9 (C-2′), 166.2 (C-3); ESI-MS 449 $[M+H]^+$; Anal. Calcd. for $C_{26}H_{32}N_4OS$ C 69.61; H 7.19. Found C 69.75; H 7.06.

*4.2.2.11. 17β-Hydroxy-7′-methyl-[1,2,4]triazolo[1,5-a]pyrimidino[5′,6′:3,2]-5α-androstane (**8k**).* Substrate: **2k** [21] (316 mg); Reagent: 3AT (168 mg). For purification of the crude product, EtOAc/CH_2Cl_2 = 50:50 eluent was used. Yield: 261 mg (69 %, white solid); Mp > 200 °C (decomp.); ^{1}H NMR ($CDCl_3$, 500 MHz): δ 0.79 (s, 3H, 18-H_3), 0.82 (s, 3H, 19-H_3), 0.86–1.05 (overlapping m, 3 H), 1.16 (m, 1 H), 1.27–1.57 (overlapping m, 5 H), 1.61–1.81 (overlapping m, 5 H), 1.91 (m, 1 H), 2.09 (m, 1 H), 2.37 (d, 1H, *J* =16.0 Hz, 1α-H), 2.77 (dd, 1H, *J* =19.3 Hz, *J* =13.0 Hz, 4β-H), 2.78 (s, 3H, 7′−CH_3), 2.89 (d, 1H, *J* =16.0 Hz, 1β-H), 3.02 (dd, 1H, *J* =19.3 Hz, *J* = 5.1 Hz, 4α-H), 3.68 (t, 1H, *J* =8.6 Hz, 17α-H), 8.42 (s, 1H, 2′-H); ^{13}C NMR ($CDCl_3$, 125 MHz): δ 11.2 (C-18), 12.2 (C-19), 13.8 (7′−CH_3), 21.1 (C-11), 23.5 (C-15), 28.3 (C-6), 30.7 (C-16), 31.1 (C-7), 35.1 (C-10), 35.7 (C-8), 36.8 (C-12), 37.4 (C-4), 39.3 (C-1), 41.3 (C-5), 43.0 (C-13), 51.1 (C-14), 54.0 (C-9), 82.0 (C-17), 118.0 (C-2), 145.4 (C-7′), 152.9 (C-3a'), 154.4 (C-2′) 164.7 (C-3); ESI-MS 381 $[M+H]^+$; Anal. Calcd. for $C_{23}H_{32}N_4O$ C 72.60; H 8.48. Found C 72.55; H 8.32.

4.2.3. General procedure for the synthesis of heterocyclic 17-keto steroids by Jones oxidation

The crude product (**6a**, **7a**, **8a**–**f** or **8i-k**) of the heterocyclization (*4.2.2.*) was dissolved in acetone (10 mL) and Jones reagent (0.2 mL) was added dropwise into the solution, which was then stirred at room temperature for 30 min, after which it was poured into ice-cold water. NH_4Cl was added and the resulting precipitate was filtered off and dried. The crude product was purified by column chromatography.

*2-Methyl-7′-phenylpyrazolo[1′,5′-a]pyrimidino[5′,6′:3,2]-5α-androstan-17-one(**9a**).* Yield: 241 mg (53 %, off white solid); Mp > 250 °C (decomp.); ^{1}H NMR ($CDCl_3$, 500 MHz): δ 0.76 (s, 3H, 19-H_3), 0.83 (s, 3H, 18-H_3), 0.87 (m, 1 H), 1.06 (m, 1 H), 1.20 (m, 1 H), 1.31–1.41 (overlapping m, 4 H), 1.49–1.57 (overlapping m, 2 H), 1.69–1.77 (m, overlapping m, 3 H), 1.88 (m, 1 H), 1.96 (m, 1 H), 2.07 (m, 1H, 16α-H), 2.21 (d, 1H, *J* =16.0 Hz, 1α -H), 2.41 (s, 3H, 2′−CH_3), 2.44 (dd, 1H, *J* =19.0 Hz, *J* =8.6 Hz, 16β-H), 2.56 (d, 1H, *J* =16.0 Hz, 1β-H), 2.75 (dd, 1H, *J* =19.0 Hz, *J* =12.5 Hz, 4β-H), 3.09 (dd, 1H, *J* =16.0 Hz, *J* = 5.3 Hz, 4α-H), 6.43 (s, 1H, 3′-H), 7.45 (bs, 2H, 2″-H and 6″-H), 7.54–7.60 (m, 3H, 3″-H, 4″-H and 5″-H); ^{13}C NMR ($CDCl_3$, 125 MHz): δ 11.7 (C-19), 13.8 (C-18), 15.0 (2′−CH_3), 20.5 (C-11), 21.9 (C-15), 28.3 (C-6), 29.8 (CH_2), 30.4 (CH_2), 31.5 (CH_2), 35.2 (C-8), 35.5 (C-10), 35.9 (C-4), 39.9 (C-1), 41.5 (C-5), 47.7 (C-13), 51.4 (C-14), 53.5 (C-9), 94.1 (C-3′), 113.9 (C-2), 114.2 (C-3a'), 129.1 (2C) and 129.3 (2C): C-2″, C-6″, C-3″ and C-5″, 130.1 (C-1″), 130.4 (C-4″), 158.0 (C-3), 221.1 (C-17), the signal for C-7′ carbonyl-C was not observed owing to the long relaxation time of this carbon nucleus; ESI-MS 440 $[M+H]^+$; Anal. Calcd. for $C_{29}H_{33}N_3O$ C 79.23; H 7.57. Found C 79.11; H 7.47.

*4.2.3.2. 7′-Phenylpyrazolo[1′,5′-a]pyrimidino[5′,6′:3,2]-5α-androstan-17-one(**10a**).* Yield: 237 mg (54 %, yellow solid); Mp > 250 °C (decomp.); ^{1}H NMR ($CDCl_3$, 500 MHz): δ 0.79 (s, 3H, 19-H_3), 0.84 (s, 3H, 18-H_3), 0.86 (m, 1 H), 1.06 (m, 1 H), 1.20 (m, 1 H), 1.31–1.42 (overlapping m, 4 H), 1.50–1.57 (overlapping m, 2 H), 1.72–1.78 (m, overlapping m, 3 H), 1.89 (m, 1 H), 1.97 (m, 1 H), 2.07 (m, 1H, 16α-H), 2.25 (d, 1H, *J* =16.1 Hz, 1α -H), 2.44 (dd, 1H, *J* =19.2 Hz, *J* =8.6 Hz, 16β-H),

2.65 (d, 1H, J =16.1 Hz, 1β-H), 2.78 (dd, 1H, J =19.2 Hz, J =12.7 Hz, 4β-H), 3.11 (dd, 1H, J =19.2 Hz, J = 5.6 Hz, 4α-H), 6.62 (bs, 1H, 3′-H), 7.45 (bd, 2H, 2″-H and 6″-H), 7.54–7.61 (m, 3H, 3″-H, 4″-H and 5″-H), 7.99 (d, 1H, J =2.2 Hz, 2′-H); ^{13}C NMR ($CDCl_3$, 125 MHz): δ 11.8 (C-19), 13.8 (C-18), 20.6 (C-11), 21.9 (C-15), 28.4 (C-6), 30.5 (CH_2), 31.6 (CH_2), 35.3 (C-8), 35.6 (C-10), 35.9 (C-4), 36.8 (CH_2), 40.0 (C-1), 41.8 (C-5), 47.7 (C-13), 51.6 (C-14), 53.7 (C-9), 94.9 (C-3′), 114.9 (C-2), 129.2 (2C) and 129.3 (2C): C-2″, C-6″, C-3″ and C-5″, 130.3 (C-1″), 130.4 (C-4″), 144.9 (C-2′), 145.8 and 147.0 (C-3a' and C-7′), 158.7 (C-3), 220.6 (C-17); ESI-MS 440 $[M+H]^+$; Anal. Calcd. for $C_{29}H_{33}N_3O$ C 79.23; H 7.57. Found C 79.11; H 7.47.

*4.2.3.3. 7′-Phenyl-[1,2,4]triazolo[1,5-a]pyrimidino[5′,6′:3,2]-5α-androstan-17-one (**11a**).* Yield: 258 mg (59 %, white solid); Mp > 300 °C (decomp.); ^{1}H NMR ($CDCl_3$, 500 MHz): δ 0.78 (s, 3H, 19-H_3), 0.84 (s, 3H, 18-H_3), 0.90 (m, 1 H), 1.08 (m, 1 H), 1.19–1.44 (overlapping m, 5 H), 1.49–1.60 (overlapping m, 2 H), 1.78 (overlapping m, 3 H), 1.90 (m, 1 H), 1.98 (m, 1 H), 2.08 (m, 1H, 16α-H), 2.37 (d, 1H, J =16.3 Hz, 1α-H), 2.46 (dd, 1H, J =19.2 Hz, J =8.8 Hz, 16β-H), 2.74 (d, 1H, J =16.3 Hz, 1β-H), 2.85 (dd, 1H, J =19.6 Hz, J =12.6 Hz, 4β-H), 3.20 (dd, 1H, J =19.6 Hz, J = 5.4 Hz, 4α-H), 7.50 (m, 2H, 2″-H és 6″-H), 7.63 (m, 3H, 3″-H, 4″-H and 5″-H), 8.42 (s, 1H, 2′-H); ^{13}C NMR ($CDCl_3$, 125 MHz): δ 11.8 (C-19), 13.8 (C-18), 20.6 (CH_2), 21.9 (CH_2), 28.2 (C-6), 30.4 (CH_2), 31.5 (CH_2), 35.2 (C-8), 35.4 (C-10), 35.9 (CH_2), 37.7 (C-4), 40.0 (C-1), 41.4 (C-5), 47.6 (C-13), 51.4 (C-14), 53.5 (C-9), 119.2 (C-2), 128.4 (C-1″), 129.3 (4C, C-2″, C-3″, C-5″ and C-6″), 131.3 (C-4″), 146.7 (C-7′), 151.8 (C-3a'), 152.9 (C-2′), 167.5 (C-3), 220.7 (C-17); ESI-MS 441 $[M+H]^+$; Anal. Calcd. for $C_{28}H_{32}N_4O$ C 76.33; H 7.32. Found C 76.19; H 7.45.

*4.2.3.4. 7′-(4″-Tolyl)-[1,2,4]triazolo[1,5-a]pyrimidino[5′,6′:3,2]-5α-androstan-17-one (**11b**).* Yield: 284 mg (62 %, white solid); Mp 283−286 °C; ^{1}H NMR ($CDCl_3$, 500 MHz): δ 0.78 (s, 3H, 19-H_3), 0.85 (s, 3H, 18-H_3), 0.90 (m, 1 H), 1.09 (m, 1 H), 1.21–1.60 (overlapping m, 7 H), 1.74–1.80 (overlapping m, 3 H), 1.92 (m, 1 H), 1.98 (m, 1 H), 2.09 (m, 1H, 16α-H), 2.38 (d, 1H, J =16.2 Hz, 1α-H), 2.46 (dd, 1H, J =19.2 Hz, J =8.5 Hz, 16β-H), 2.49 (s, 3H, 4″−CH_3), 2.78 (d, 1H, J =16.2 Hz, 1β-H), 2.85 (dd, 1H, J =19.6 Hz, J =12.7 Hz, 4β-H), 3.20 (dd, 1H, J =19.6 Hz, J = 5.4 Hz, 4α-H), 7.39–7.44 (overlapping m, 4H, 2″-H, 3″-H, 5″-H and 6″-H), 8.43 (bs, 1H, 2′-H); ^{13}C NMR ($CDCl_3$, 125 MHz): δ 11.8 (C-19), 13.8 (C-18), 20.7 (CH_2), 21.8 (4″−CH_3), 21.9 (CH_2), 28.2 (C-6), 30.4 (CH_2), 31.5 (CH_2), 35.2 (C-8), 35.4 (C-10), 35.9 (CH_2), 37.7 (C-4), 40.1 (C-1), 41.4 (C-5), 47.6 (C-13), 51.4 (C-14), 53.5 (C-9), 119.1 (C-2), 125.3 (C-1″), 129.2 (2C, C-2″ and C-6″), 130.0 (2C, C-3″ and C-5″), 141.8 (C-4″), 146.9 (C-7′), 151.8 (C-3a'), 152.8 (C-2′), 167.3 (C-3), 220.8 (C-17); ESI-MS 455 $[M+H]^+$; Anal. Calcd. for $C_{29}H_{34}N_4O$ C 76.62; H 7.54. Found C 76.76; H 7.41.

*4.2.3.5. 7′-(3″-Tolyl)-[1,2,4]triazolo[1,5-a]pyrimidino[5′,6′:3,2]-5α-androstan-17-one (**11c**).* Yield: 301 mg (66 %, white solid); Mp 263−265 °C; ^{1}H NMR ($CDCl_3$, 500 MHz): δ 0.79 (s, 3H, 19-H_3), 0.85 (s, 3H, 18-H_3), 0.89 (m, 1 H), 1.07 (m, 1 H), 1.20–1.60 (overlapping m, 7 H), 1.73–1.81 (overlapping m, 3 H), 1.89–2.00 (overlapping m, 2 H), 2.08 (m, 1H, 16α-H), 2.32 (d, 1H, J =16.2 Hz, 1α-H), 2.45 (dd, 1H, J =19.2 Hz, J =8.6 Hz, 16β-H), 2.47 (s, 3H, 3″−CH_3), 2.72 (d, 1H, J =16.2 Hz, 1β-H), 2.83 (dd, 1H, J =19.5 Hz, J =12.7 Hz, 4β-H), 3.17 (dd, 1H, J =19.5 Hz, J = 5.5 Hz, 4α-H), 7.26 (m, 2 H), 7.41 (d-like m, 1 H): 2″-H, 4″-H and 6″-H, 7.50 (t-like m, 1H, 5″-H), 8.35 (s, 1H, 2′-H); ^{13}C NMR ($CDCl_3$, 125 MHz): δ 11.8 (C-19), 13.8 (C-18), 20.6 (CH_2), 21.7 (3″−CH_3), 21.9 (CH_2), 28.3 (C-6), 30.4 (CH_2), 31.5 (CH_2), 35.2 (C-8), 35.4 (C-10), 35.9 (CH_2), 37.6 (C-4), 40.0 (C-1), 41.5 (C-5), 47.7 (C-13), 51.4 (C-14), 53.5 (C-9), 117.9 (C-2), 126.1 (C-6″), 129.0 (C-1″), 129.2, 129.5 and 131.8 (C-2″, C-4″ and C-5″), 139.2 (C-4″), 146.5 (C-7′), 153.7 (C-3a'), 155.2 (C-2′), 165.6 (C-3), 220.9 (C-17); ESI-MS 455 $[M+H]^+$; Anal. Calcd. for $C_{29}H_{34}N_4O$ C 76.62; H 7.54. Found C 76.55; H 7.60.

*4.2.3.6. 7′-(4″-Methoxyphenyl)-[1,2,4]triazolo[1,5-a]pyrimidino[5′,6′:3,2]-5α-androstan-17-one (**11d**).* Yield: 280 mg (59 %, white solid); Mp 273−275 °C; ^{1}H NMR ($CDCl_3$, 500 MHz): δ 0.76 (s, 3H, 19-H_3), 0.85 (s, 3H, 18-H_3), 0.91 (m, 1 H), 1.08 (m, 1 H), 1.22–1.42 (overlapping m, 5 H), 1.47–1.60 (overlapping m, 2 H), 1.73–1.80 (overlapping m, 3 H), 1.91 (m, 1 H), 1.98 (m, 1 H), 2.09 (m, 1H, 16α-H), 2.40 (d, 1H, J =16.2 Hz, 1α-H), 2.46 (dd, 1H, J =19.2 Hz, J =8.8 Hz, 16β-H), 2.79 (d, 1H, J =16.2 Hz, 1β-H), 2.83 (dd, 1H, J =19.6 Hz, J =12.6 Hz, 4β-H), 3.19 (dd, 1H, J =19.6 Hz, J = 5.3 Hz, 4α-H), 3.92 (s, 3H, 4″-OMe), 7.13 (d, 2H, J =8.7 Hz, 3″-H and 5″-H), 7.49 (d, 2H, J =8.7 Hz, 2″-H and 6″-H), 8.42 (bs, 1H, 2′-H); ^{13}C NMR ($CDCl_3$, 125 MHz): δ 11.8 (C-19), 13.8 (C-18), 20.7 (CH_2), 21.9 (CH_2), 28.1 (C-6), 30.4 (CH_2), 31.5 (CH_2), 35.2 (C-8), 35.4 (C-10), 35.9 (CH_2), 37.7 (C-4), 40.z2 (C-1), 41.4 (C-5), 47.7 (C-13), 51.4 (C-14), 53.5 (C-9), 55.6 (4″-OMe), 114.6 (2C, C-3″ and C-5″), 118.7 (C-2), 120.2 (C-1″), 131.2 (2C, C-2″ and C-6″), 146.5 (C-7′), 152.2 (C-3a'), 153.3 (C-2′), 161.6 (C-4″), 166.9 (C-3), 221.0 (C-17); ESI-MS 471 $[M+H]^+$; Anal. Calcd. for $C_{29}H_{34}N_4O_2$ C 74.01; H 7.28. Found C 74.15; H 7.17.

*4.2.3.7. 7′-(4″-Fluorophenyl)-[1,2,4]triazolo[1,5-a]pyrimidino[5′,6′:3,2]-5α-androstan-17-one (**11e**).* Yield: 261 mg (57 %, white solid); Mp > 250 °C (decomp.); ^{1}H NMR ($CDCl_3$, 500 MHz): δ 0.78 (s, 3H, 19-H_3), 0.85 (s, 3H, 18-H_3), 0.90 (m, 1 H), 1.08 (m, 1 H), 1.21–1.47 (overlapping m, 5 H), 1.51–1.61 (overlapping m, 2 H), 1.73–1.93 (overlapping m, 4 H), 1.98 (m, 1 H), 2.08 (m, 1H, 16α-H), 2.35 (d, 1H, J =16.2 Hz, 1α-H), 2.46 (dd, 1H, J =19.2 Hz, J =8.7 Hz, 16β-H), 2.70 (d, 1H, J =16.2 Hz, 1β-H), 2.83 (dd, 1H, J =19.2 Hz, J =12.9 Hz, 4β-H), 3.17 (dd, 1H, J =19.2 Hz, J = 5.5 Hz, 4α-H), 7.31 (m, 2H, 3″-H and 5″-H), 7.51 (m, 2H, 2″-H and 6″-H), 8.34 (s, 1H, 2′-H); ^{13}C NMR ($CDCl_3$, 125 MHz): δ 11.8 (C-19), 13.8 (C-18), 20.7 (CH_2), 21.9 (CH_2), 28.2 (C-6), 30.4 (CH_2), 31.5 (CH_2), 35.2 (C-8), 35.5 (C-10), 35.9 (CH_2), 37.6 (C-4), 40.1 (C-1), 41.5 (C-5), 47.7 (C-13), 51.4 (C-14), 53.6 (C-9), 116.6 (d, 2C, J =22.1 Hz, C-3″ and C-5″), 117.8 (C-2), 125.0 (d, J =3.6 Hz, C-1″), 131.7 (d, 2C, J =8.7 Hz, C-2″ and C-6″), 145.1 (C-7′), 154.0 (C-3a'), 155.5 (C-2′), 164.0 (d, J =252.0 Hz, C-4″), 165.5 (C-3) 220.8 (C-17); ESI-MS 459 $[M+H]^+$; Anal. Calcd. for $C_{28}H_{31}FN_4O$ C 73.34; H 6.81. Found C 73.28; H 6.74.

*4.2.3.8. 7′-(4″-Chlorophenyl)-[1,2,4]triazolo[1,5-a]pyrimidino[5′,6′:3,2]-5α-androstan-17-one (**11f**).* Yield: 293 mg (62 %, white solid); Mp > 300 °C (decomp.); ^{1}H NMR ($CDCl_3$, 500 MHz): δ 0.78 (s, 3H, 19-H_3), 0.85 (s, 3H, 18-H_3), 0.89 (m, 1 H), 1.08 (m, 1 H), 1.21–1.61 (overlapping m, 7 H), 1.74–1.82 (overlapping m, 3 H), 1.91 (m, 1 H), 1.98 (m, 1 H), 2.09 (m, 1H, 16α-H), 2.37 (d, 1H, J =16.2 Hz, 1α-H), 2.46 (dd, 1H, J =19.2 Hz, J =8.8 Hz, 16β-H), 2.72 (d, 1H, J =16.2 Hz, 1β-H), 2.85 (dd, 1H, J =19.6 Hz, J =12.6 Hz, 4β-H), 3.20 (dd, 1H, J =19.6 Hz, J = 5.3 Hz, 4α-H), 7.47 (d, 2H, J =8.2 Hz, 3″-H and 5″-H), 7.61 (d, 2H, J = 2″-H and 6″-H), 8.40 (bs, 1H, 2′-H); ^{13}C NMR ($CDCl_3$, 125 MHz): δ 11.9 (C-19), 13.8 (C-18), 20.7 (CH_2), 21.9 (CH_2), 28.2 (CH_2), 30.4 (CH_2), 31.5 (CH_2), 35.2 (C-8), 35.5 (C-10), 35.9 (CH_2), 37.7 (C-4), 40.1 (C-1), 41.4 (C-5), 47.6 (C-13), 51.4 (C-14), 53.5 (C-9), 118.8 (C-2), 126.9 (C-1″), 129.7 (2C, C-2″ and C-6″), 130.9 (2C, C-3″ and C-5″), 137.5 (C-4″), 145.2 (C-7′), 152.6 (C-3a'), 153.8 (C-2′), 166.8 (C-3), 220.7 (C-17); ESI-MS 475 $[M+H]^+$; Anal. Calcd. for $C_{28}H_{31}ClN_4O$ C 70.80; H 6.58. Found C 70.71; H 6.45.

*4.2.3.9. 7′-(Furan-2″-yl)-[1,2,4]triazolo[1,5-a]pyrimidino[5′,6′:3,2]-5α-androstan-17-one (**11i**).* Yield: 238 mg (55 %, light brown solid); Mp > 200 °C (decomp.); ^{1}H NMR ($CDCl_3$, 500 MHz): δ 0.81 (s, 3H, 19-H_3), 0.90 (s, 3H, 18-H_3), 1.03 (m, 1 H), 1.12 (m, 1 H), 1.32–1.65 (overlapping m, 7 H), 1.74–1.83 (overlapping m, 3 H), 1.92 (m, 1 H), 2.01 (m, 1 H), 2.12 (m, 1H, 16α-H), 2.48 (dd, 1H, J =19.4 Hz, J =8.7 Hz, 16β-H), 2.78 (d, 1H, J =17.1 Hz, 1α-H), 2.87 (dd, 1H, J =19.4 Hz, J =12.6 Hz, 4β-H), 3.13 (dd, 1H, J =19.4 Hz, J = 5.3 Hz, 4α-H), 3.38 (d, 1H, J =17.1 Hz, 1β-H), 6.79 (dd, 1H, J =3.6 Hz, J =1.7 Hz, 4″-H), 7.86 (d, 1H, J =1.7 Hz, 3″-

Table 4
Crystal data and structure refinement for compounds **2a** and **8j.**

	2a	**8j**
Empirical formula	$C_{26}H_{34}O_2$	$C_{53}H_{66}Cl_2N_8O_2S_2$
Molecular formula	$C_{26}H_{34}O_2$	2 ($C_{26}H_{32}N_4OS$) CH_2Cl_2
Formula weight	378.53	982.15
Temperature (K)	153(2)	153(2)
Radiation and wavelength λ (Å)	Mo-*Kα*, 0.71073	Mo-*Kα*, 0.71075
Crystal system	monoclinic	monoclinic
Space group	*P* 2_1	*P* 2_1
Unit cell dimensions		
a (Å)	7.0071(5)	12.4299(8)
b (Å)	12.0136(9)	11.2453(7)
c (Å)	12.7119(10)	17.5904(11)
β (°)	95.767(7)	92.572(7)
Volume Å^3	1064.68(14)	2456.3(3)
Z	2/1	2/1
Density (calculated) (Mg/m^3)	1.181	1.328
Absorption coefficient, μ (mm^{-1})	0.072	0.268
F(000)	412	1044
Crystal colour	colourless	colourless
Crystal description	block	chunk
Crystal size (mm)	0.50 × 0.50 × 0.50	0.35 × 0.30 × 0.30
Absorption correction	numerical	numerical
Max. and min. transmission	0.981, 0.987	0.989, 0.994
θ−range for data collection (°)	3.192 ≤ θ ≤ 30.480	3.281 ≤ θ ≤ 25.347°
Reflections collected	26,315	31,944
Completeness to 2θ	0.999	0.997
Independent reflections (*R*(int))	6433 (0.0250)	8944 (0.0587)
Reflections $I>2\sigma(I)$	5960	7107
Refinement method	full-matrix least-squares on F^2	full-matrix least-squares on F^2
Data / restraints / parameters	6433 /1 /260	8944 /1 /605
Goodness-of-fit on *F*2	1.081	1.018
Final *R* indices [$I>2\sigma(I)$], R_1, wR_2	0.0407, 0.0945	0.0474, 0.0849
R indices (all data), R_1, wR_2	0.0449, 0.0962	0.0676, 0.0905
Max. and mean shift/esd	0.000; 0.000	0.001; 0.000
Largest diff. peak and hole (e. Å^{-3})	0.417; -0.145	0.423; -0.380

H), 8.14 (d, 1H, *J* =3.6 Hz, 5″-H), 8.53 (s, 1H, 2′-H); ^{13}C NMR ($CDCl_3$, 125 MHz): δ 12.0 (C-19), 13.9 (C-18), 20.9 (CH_2), 22.0 (CH_2), 28.1 (CH_2), 30.4 (CH_2), 31.7 (CH_2), 35.1 (C-10), 35.2 (C-8), 36.0 (CH_2), 37.8 (C-4), 40.6 (C-1), 40.7 (C-5), 47.7 (C-13), 51.5 (C-14), 54.0 (C-9), 112.8 (C-3″), 117.2 (C-2), 122.3 (C-4″), 135.6 (C-2″), 143.7 (C-7′), 146.3 (C-5″), 152.7 (C-3a'), 153.7 (C-2′), 166.1 (C-3), 221.0 (C-17); ESI-MS 431 $[M+H]^+$; Anal. Calcd. for $C_{26}H_{30}N_4O_2$ C 72.53; H 7.02. Found C 72.41; H 6.94.

4.2.3.10. 7′-(Thiophen-2″-yl)-[1,2,4]triazolo[1,5-a]pyrimidino [5′,6′:3,2]-5α-androstan-17-one ***(11j)***. Yield: 264 mg (57 %, yellow solid); Mp > 300 °C (decomp.); ^{1}H NMR ($CDCl_3$, 500 MHz): δ 0.77 (s, 3H, 19-H_3), 0.87 (s, 3H, 18-H_3), 0.98 (m, 1 H), 1.10 (m, 1 H), 1.29–1.66 (overlapping m, 7 H), 1.74–1.86 (overlapping m, 3 H), 1.93 (m, 1 H), 2.00 (m, 1 H), 2.11 (m, 1H, 16α-H), 2.47 (dd, 1H, *J* =19.1 Hz, *J* =8.9 Hz, 16β-H), 2.56 (d, 1H, *J* =16.1 Hz, 1α-H), 2.85 (dd, 1H, *J* =19.6 Hz, *J* =12.6 Hz, 4β-H), 3.09 (d, 1H, *J* =16.1 Hz, 1β-H), 3.18 (dd, 1H, *J* =19.6 Hz, *J* = 5.5 Hz, 4α-H), 7.33 (t, 1H, *J* =4.4 Hz, 4″-H), 7.80 (m, 2H, 3″-H and 5″-H), 8.47 (s, 1H, 2′-H); ^{13}C NMR ($CDCl_3$, 125 MHz): δ 11.8 (C-19), 13.8 (C-18), 20.9 (CH_2), 21.9 (CH_2), 28.1 (CH_2), 30.4 (CH_2), 31.6 (CH_2), 35.2 (C-8), 35.6 (C-10), 35.9 (CH_2), 37.7 (C-4), 41.2 (C-5), 41.3 (C-1), 47.7 (C-13), 51.4 (C-14), 53.7 (C-9), 118.6 (C-2), 127.5 (C-3″), 127.8 (C-2″), 131.6 (C-4″), 134.1 (C-5″), 140.6 (C-7′), 152.7 (C-3a'), 153.7 (C-2′), 166.2 (C-3) 221.0 (C-17); ESI-MS 447 $[M+H]^+$; Anal. Calcd. for $C_{26}H_{30}N_4OS$ C 69.92; H 6.77. Found C 70.05; H 6.65.

7′-Methyl-[1,2,4]triazolo[1,5-a]pyrimidino[5′,6′:3,2]-5α-androstan-17-one ***(11k)***. Yield: 197 mg (52 %, white solid); Mp > 250 °C (decomp.); ^{1}H NMR ($CDCl_3$, 500 MHz): δ 0.84 (s, 3H, 19-H_3), 0.91 (s, 3H, 18-H_3), 0.98 (m, 1 H), 1.09 (m, 1 H), 1.30–1.44 (overlapping m, 3 H), 1.51–1.65 (overlapping m, 3 H), 1.69–1.76 (overlapping m, 2 H), 1.82 (m, 1 H), 1.92 (m, 2 H), 2.00 (m, 1 H), 2.10 (m, 1H, 16α-H), 2.39 (d, 1H, *J* =16.0 Hz, 1α-H), 2.48 (dd, 1H, *J* =19.3 Hz, *J* =8.7 Hz, the 16β-H), 2.79 (s, 3H, 7′−CH_3 and m, 1H, 4β-H), 2.90 (d, 1H, *J* =16.2 Hz, 1β-H), 3.04 (dd, 1H, *J* =19.4 Hz, *J* = 5.1 Hz, 4α-H), 8.44 (s, 1H, 2′-H); ^{13}C NMR ($CDCl_3$, 125 MHz): δ 12.1 (C-19), 13.8 (7′−CH_3), 13.9 (C-18), 20.8 (CH_2), 21.9 (CH_2), 28.1 (C-6), 30.4 (CH_2), 31.6 (CH_2), 35.2 (C-8), 35.9 (2C, C-10 and CH_2), 37.3 (C-4), 39.2 (C-1), 41.2 (C-5), 47.7 (C-13), 51.5 (C-14), 51.9 (C-9), 118.1 (C-2), 145.6 (C-7′), 152.4 (C-3a'), 153.9 (C-2′), 164.9 (C-3), 220.8 (C-17); ESI-MS 379 $[M+H]^+$; Anal. Calcd. for $C_{23}H_{30}N_4O$ C 72.98; H 7.99. Found C 73.12; H 7.89.

4.3. X-ray data collection, structure solution and refinement for compound ***2a*** *and* ***8j***

Single crystals suitable for single crystal X-ray diffraction measurements have been obtained by evaporation from methanol, resulting in crystal **2a** and from CH_2Cl_2/diethyl-ether leading to crystal **8 j**. The crystals were mounted on loops and X-ray diffraction data were collected at 153(2) K on a Rigaku RAXIS-RAPID II diffractometer using Mo-*Kα* radiation. Numerical absorption correction [39] was carried out using the program CrystalClear [40] SHELX [41] program package under WinGX [42] software were used for structure solution and refinement. The structures were solved by direct methods. The models were refined by full-matrix least squares on F^2. Refinement of non-hydrogen atoms was carried out with anisotropic temperature factors (except for disordered carbon atoms C23A and C23B in crystal **8 j** where isotropic temperature factor was used). Hydrogen atoms were placed into geometric positions. They were included in structure factor calculations but they were not refined. The isotropic displacement parameters of all the hydrogen atoms were approximated from the U(eq) value of the atom they were bonded to. In crystal **8 j**, two molecules and one dichloromethane have been found in the asymmetric unit. In molecule 2 the thiophene rings was found in two disordered positions

with an occupancy of 76 % for C23A and S21A and 24 % for C23B and S21B atoms. Constrains have been used for the refinement of the position and ADP of disordered atoms. As the configuration of the chiral atoms of DHT was known and the reactions did not lead to novel asymmetric center, the absolute configuration was not investigated. The summary of data collection and refinement parameters are collected in Table 4. Selected bond lengths and angles of compounds calculated by PLATON software [43] are collected in **Tables S1** and **S2**. The graphical representation and the edition of CIF files were done by Mercury [44] and EnCIFer [45] softwares. The crystallographic data files for the two compounds have been deposited with the Cambridge Crystallographic Database as CCDC 2062396-2062397.

4.4. Cell lines

The 22Rv1-ARE14 reporter cell line [29] and C4-2 were kindly provided by prof. Zdeněk Dvořák and by Dr. Marián Hajdúch, respectively (both from Palacký University Olomouc, Czech Republic). 22Rv1-ARE14 and C4-2 cell lines were grown in RPMI-1640 medium. All media were supplemented with 10 % normal or charcoal-stripped fetal bovine serum (steroid-depleted serum), 4 mM glutamine, 100 IU/mL penicillin, 100 mg/mL streptomycin and 1 mM sodium pyruvate. Cells were cultivated in a humidified incubator at 5% CO_2 atmosphere and 37 °C.

4.5. AR-transcriptional luciferase assay

22Rv1-ARE14 cells were seeded into the Nunc™ MicroWell™ 96-well optical-bottom plate (Thermo Fisher Scientific) (40 000 cells/well). The next day, the cultivation medium was discarded and cells were washed with PBS. Cells were then incubated in the absence or presence of tested compounds dissolved in RPMI-1640 medium supplemented with charcoal-stripped serum and 1 nM R1881. After 24 h incubation, cells were washed with PBS and lysed for 10 min in a lysis buffer (10 mM Tris pH = 7.4, 2 mM DCTA, 1% nonidet P40, 2 mM DTT) at 37 °C. After lysis, reaction buffer (20 mM tricine pH = 7.8, 1.07 mM $MgSO4 \cdot 7H_20$, 5 mM ATP, 9.4 mM luciferin) was added to the wells and the luminescence of the samples was measured using a Tecan M200Pro microplate reader (Biotek). Assays were performed in triplicate.

4.6. Cell viability assay

For the viability assays, 22Rv1-ARE14 (10000 cells per well) and C4−2 (5000 cells per well)were seeded into the 96-well tissue culture plates and were cultivated overnight. Solutions of analysed compounds were then added in different concentrations in triplicate for 72 h. After treatment, the resazurin solution (Sigma Aldrich) was added to a final concentration of 10 μg per ml for 4 h, and then the fluorescence of resorufin was measured at 544 nm/590 nm (excitation/emission) using a Fluoroskan Ascent microplate reader (Labsystems). Finally, GI_{50} value was calculated from the dose response curves that resulted from the assays using GraphPad Prism 5.

4.7. Colony formation assay

PCa cells 22Rv1-ARE14 (2000 cells per well) and C4-2 (5000 cells per well) were seeded into 6-well plates and cultivated overnight. The following day, the medium was removed and replaced with fresh medium containing different concentrations of the compound. Media containing compounds were replaced once within 10 days. After that, the medium was discarded and colonies were fixed with 70 % ethanol for 15 min, washed with PBS and stained with crystal violet (1 % solution in 96 % ethanol) for 1 h. Finally, wells were washed with PBS until colonies were visible and its photograph was captured.

4.8. Thermal shift assay

CETSA experiment was inspired by published protocol [30,31]. C4-2 cells were deprived of androgens (by cultivation in charcoal stripped serum for 24 h), then were harvested, washed twice with PBS and treated with R1881 or several concentrations of **2f** for 1 h at 37 °C in PBS with 5 mM glucose. Following the incubation the treated cells were aliquoted into PCR strips and heated at different temperatures for 3 min in CFX96 Touch Real-time PCR detection system (BioRad). Finally, all samples were supplemented with protease inhibitors and lysed by freeze-thaw cycles using liquid nitrogen. Samples were clarified by centrifugation at 14000 *g* for 20 min and supernatants were collected and denaturated and separated by SDS-PAGE and immunoblotted.

4.9. Immunoblotting

Briefly, the cells were harvested and lysed using standard protocol in RIPA buffer supplemented with protease and phosphatase inhibitors. Cells were also disrupted by ultrasound sonication (10 s with 30 % amplitude). Cellular fractionation was performed using the Qproteome Cell Compartment Kit (Qiagen). Protein concentration was balanced within samples and then proteins were separated by SDS-PAGE and electrobloted onto nitrocellulose membranes. Membranes were blocked in 4% BSA and incubated with primary antibodies overnight. The next day, membranes were washed and incubated with secondary antibodies conjugated with peroxidase. Then, peroxidase activity was detected by SuperSignal West Pico reagents (Thermo Scientific) using a CCD camera LAS-4000 (Fujifilm). Specific antibodies were purchased from Merck (anti-α-tubulin, clone DM1A; anti phospho-histone H3 (Ser10); anti-β-actin, clone C4), or Cell Signaling Technology (anti-AR, clone D6F11; anti-PSA/KLK3, clone D6B1; anti-Nkx3.1, clone D2Y1A; anti-PARP, clone 46D11; anti-rabbit secondary antibody). All antibodies were diluted in 4% BSA and 0.1 % Tween 20 in TBS.

4.10. Molecular docking

Molecular docking is useful theoretical method for prediction and interpretation of new designed derivatives based on dihydrotestosterone ligand. Androgen receptor PDBID:2PIV [36] was selected as crystal structure as an input to molecular docking. The docking studies were performed using AutoDock Vina 1.05 [37]. Amino acids up to 6 Å from the active site were set as flexible. These settings enabled amino acid movement, increased the permitted volume of active site, and allowed the placement of DHT derivatives into the otherwise smaller highly-packed cavity for native ligands (*e.g.* DHT). All 3D structures of DHT derivatives were obtained with Marvin 15.1.5, a software used for the drawing, displaying and characterization of chemical structure, substructures and reactions. Polar hydrogens were added to all ligands and proteins with the AutoDock Tools (ADT) [38] program prior to docking with Autodock Vina program.

Author statement

Conceptualization, É.F. and R.J.; Chemical synthesis and optimization experiments, M.A.K. and Á.B.; Pharmacological studies, M.P.; Single crystal X-ray analysis, N.V.M.; Flexible docking, V.B.; Structural analysis, M.A.K.; Formal analysis and interpretation of data, Á.B. and M. P.; Methodology, resources, supervision, É.F. and R.J.; Writing—original draft preparation, M.P., N.V.M. and M.A.K.; Writing—review and editing, É.F. and R.J. All authors have read and agreed to the published version of the manuscript.

Acknowledgement

N.V.M. thanks the financial support for the National Research, Development and Innovation Office (OTKA K124544). The authors (RJ,

MP, VB) gratefully acknowledge financial support from the Grant Agency of the Czech Republic (GA20-15621S) and Palacký University Olomouc (IGA_PrF_2021_007). VB was supported by the ELIXIR CZ research infrastructure project (MEYS Grant No: LM2018131) including access to computing and storage facilities".

Appendix A. Supplementary data

Supplementary material related to this article can be found, in the online version, at doi:https://doi.org/10.1016/j.jsbmb.2021.105904.

References

[1] A. Paschalis, J.S. de Bono, Prostate cancer 2020: "The Times They Are a'Changing", Cancer Cell 38 (2020) 25–27, https://doi.org/10.1016/j.ccell.2020.06.008.
[2] S. Cao, Y. Zhan, Y. Dong, Emerging data on androgen receptor splice variants in prostate cancer, Endocr. Relat. Cancer 23 (2016) T199–T210, https://doi.org/10.1530/ERC-16-0298.
[3] C. Lu, J. Luo, Decoding the androgen receptor splice variants, Transl. Androl. Urol. 2 (2013) 178–186, https://doi.org/10.3978/j.issn.2223-4683.2013.09.08.
[4] T. Uo, S.R. Plymate, C.C. Sprenger, The potential of AR-V7 as a therapeutic target, Expert Opin. Ther. Targets 22 (2018) 201–216, https://doi.org/10.1080/14728222.2018.1439016.
[5] S. Saranyutanon, S.K. Srivastava, S. Pai, S. Singh, A.P. Singh, Therapies targeted to androgen receptor signaling axis in prostate cancer: progress, challenges, and hope, Cancers (Basel). 12 (2019) 51, https://doi.org/10.3390/cancers12010051.
[6] P. Purushottamachar, A.M. Godbole, L.K. Gediya, M.S. Martin, T.S. Vasaitis, A. K. Kwegyir-Afful, S. Ramalingam, Z. Ates-Alagoz, V.C. Njar, Systematic structure modifications of multitarget prostate cancer drug candidate galeterone to produce novel androgen receptor down-regulating agents as an approach to treatment of advanced prostate cancer, J. Med. Chem. 56 (2013) 4880–4898, https://doi.org/10.1021/jm400048v.
[7] F. Cortés-Benítez, M. Cabeza, M.T. Ramírez-Apan, B. Alvarez-Manrique, E. Bratoeff, Synthesis of 17β-*N*-arylcarbamoylandrost-4-en-3-one derivatives and their anti-proliferative effect on human androgen-sensitive LNCaP cell line, Eur. J. Med. Chem. 121 (2016) 737–746, https://doi.org/10.1016/j.ejmech.2016.05.059.
[8] Y.K. Shi, B. Wang, X.L. Shi, Y.D. Zhao, B. Yu, H.M. Liu, Synthesis and biological evaluation of new steroidal pyridines as potential anti-prostate cancer agents, Eur. J. Med. Chem. 145 (2018) 11–22, https://doi.org/10.1016/j.ejmech.2017.12.094.
[9] L.L. Romero-Hernández, P. Merino-Montiel, S. Meza-Reyes, J.L. Vega-Baez, Ó. López, J.M. Padrón, S. Montiel-Smith, Synthesis of unprecedented steroidal spiro heterocycles as potential antiproliferative drugs, Eur. J. Med. Chem. 143 (2018) 21–32, https://doi.org/10.1016/j.ejmech.2017.10.063.
[10] R. Jorda, E. Řezníčková, U. Kiełczewska, J. Maj, J.W. Morzycki, L. Siergiejczyk, V. Bazgier, K. Berka, L. Rárová, A. Wojtkielewicz, Synthesis of novel galeterone derivatives and evaluation of their *in vitro* activity against prostate cancer cell lines, Eur. J. Med. Chem. 179 (2019) 483–492, https://doi.org/10.1016/j.ejmech.2019.06.040.
[11] R. Jorda, S.M.M. Lopes, E. Řezníčková, H. Ajani, A.V. Pereira, C.S.B.M.V.D. Gomes, T. Pinho, E. Melo, Tetrahydropyrazolo[1,5-*a*]pyridine-fused steroids and their *in vitro* biological evaluation in prostate cancer, Eur. J. Med. Chem. 178 (2019) 168–176, https://doi.org/10.1016/j.ejmech.2019.05.064.
[12] V.C. Njar, A.M. Brodie, Discovery and development of Galeterone (TOK-001 or VN/124-1) for the treatment of all stages of prostate cancer, J. Med. Chem. 58 (2015) 2077–2087, https://doi.org/10.1021/jm501239f.
[13] M. Jarman, S.E. Barrie, J.M. Llera, The 16.,17-double bond is needed for irreversible inhibition of human cytochrome p45017α by abiraterone (17-(3-pyridyl)androsta-5,16-dien-3β-ol) and related steroidal inhibitors, J. Med. Chem. 41 (1998) 5375–5381, https://doi.org/10.1021/jm981017j.
[14] A.K. Kwegyir-Afful, S. Ramalingam, P. Purushottamachar, V.P. Ramamurthy, V. C. Njar, Galeterone and VNPT55 induce proteasomal degradation of AR/AR-V7, induce significant apoptosis via cytochrome c release and suppress growth of castration resistant prostate cancer xenografts *in vivo*, Oncotarget. 6 (2015) 27440–27460, https://doi.org/10.18632/oncotarget.4578.
[15] B. Montgomery, M.A. Eisenberger, M.B. Rettig, F. Chu, R. Pili, J.J. Stephenson, N. J. Vogelzang, A.J. Koletsky, L.T. Nordquist, W.J. Edenfield, K. Mamlouk, K. J. Ferrante, M.E. Taplin, Androgen receptor modulation optimized for response (ARMOR) Phase I and II studies: galeterone for the treatment of castration-resistant prostate cancer, Clin. Cancer Res. 22 (2016) 1356–1363, https://doi.org/10.1158/1078-0432.CCR-15-1432.
[16] M.E. Taplin, E.S. Antonarakis, K.J. Ferrante, K. Horgan, B. Blumenstein, F. Saad, J. Luo, J.S. de Bono, Androgen receptor modulation optimized for response-splice variant: a Phase 3, randomized trial of galeterone versus enzalutamide in androgen receptor splice variant-7-expressing metastatic castration-resistant prostate cancer, Eur. Urol. 76 (2019) 843–851, https://doi.org/10.1016/j.eururo.2019.08.034.
[17] E.A. Mostaghel, B.T. Marck, S.R. Plymate, R.L. Vessella, S. Balk, A.M. Matsumoto, P.S. Nelson, R.B. Montgomery, Resistance to CYP17A1 inhibition with abiraterone in castration-resistant prostate cancer: induction of steroidogenesis and androgen receptor splice variants, Clin. Cancer Res. 17 (2011) 5913–5925, https://doi.org/10.1158/1078-0432.CCR-11-0728.
[18] D. Kovács, J. Wölfling, N. Szabó, M. Szécsi, Z. Schelz, I. Zupkó, É. Frank, Synthesis of novel 17-(4'-formyl)pyrazolylandrosta-5,16-dienes and their derivatives as potent 17α-hydroxylase/C17,20-lyase inhibitors or antiproliferative agents depending on the substitution pattern of the heterоring, Eur. J. Med. Chem. 120 (2016) 284–295, https://doi.org/10.1016/j.ejmech.2016.05.006.
[19] D. Kovács, J. Wölfling, N. Szabó, M. Szécsi, I. Kovács, I. Zupkó, É. Frank, An efficient approach to novel 17-5′-(1′,2′,4′)-oxadiazolyl androstenes via the cyclodehydration of cytotoxic *O*-steroidacylamidoximes, and an evaluation of their inhibitory action on 17α-hydroxylase/C17,20-lyase, Eur. J. Med. Chem. 70 (2013) 649–660, https://doi.org/10.1016/j.ejmech.2013.10.038.
[20] D. Kovács, J. Wölfling, N. Szabó, M. Szécsi, R. Minorics, I. Zupkó, É. Frank, Efficient access to novel androsteno-17-(1',3',4')-oxadiazoles and 17β-(1',3',4')-thiadiazoles *via* N-substituted hydrazone and *N,N'*-disubstituted hydrazine intermediates, and their pharmacological evaluation in vitro, Eur. J. Med. Chem. 98 (2015) 13–29, https://doi.org/10.1016/j.ejmech.2015.05.010.
[21] G. Mótyán, M.K. Gopisetty, R.E. Kiss-Faludy, Á. Kulmány, I. Zupkó, É. Frank, M. Kiricsi, Anti-cancer activity of novel dihydrotestosterone-derived ring A-condensed pyrazoles on androgen non-responsive prostate cancer cell lines, Int. J. Mol. Sci. 20 (2019) 2170, https://doi.org/10.3390/ijms20092170.
[22] Á. Baji, T. Kiss, J. Wölfling, D. Kovács, N. Igaz, M.K. Gopisetty, M. Kiricsi, É. Frank, Multicomponent access to androstano-arylpyrimidines under microwave conditions and evaluation of their anti-cancer activity *in vitro*, J. Steroid Biochem. Mol. Biol. 172 (2017) 79–88, https://doi.org/10.1016/j.jsbmb.2017.06.001.
[23] P.P. Kaishap, S. Baruah, K. Shekarrao, S. Gogoi, R.C. Boruah, A facile method for the synthesis of steroidal and nonsteroidal 5-methyl pyrazolo[1,5-*a*]pyrimidines, Tetrahedron Lett. 55 (2014) 3117–3121, https://doi.org/10.1016/j.tetlet.2014.04.011.
[24] A. Arenas-González, L.A. Mendez-Delgado, P. Merino-Montiel, J.M. Padrón, S. Montiel-Smith, J.L. Vega-Báez, S. Meza- Reyes, Synthesis of monomeric and dimeric steroids containing [1,2,4]triazolo[1,5-*a*]pyrimidines, Steroids 116 (2016) 13–19, https://doi.org/10.1016/j.steroids.2016.09.014.
[25] G.M. Allan, H.R. Lawrence, J. Cornet, C. Bubert, D.S. Fischer, N. Vicker, A. Smith, H.J. Tutill, A. Purohit, J.M. Day, M.F. Mahon, M.J. Reed, B.V.L. Potter, Modification of Estrone at the 6, 16, and 17 Positions: novel potent inhibitors of 17β-hydroxysteroid dehydrogenase type 1, J. Med. Chem. 49 (2006) 1325–1345, https://doi.org/10.1021/jm050830t.
[26] V. Jeyachandran, S. Vivek Kumar, R. Ranjith Kumar, Synthesis of novel 16-spiro steroids: 7-(Aryl)tetrahydro-1*H*-pyrrolo[1,2-*c*][1,3]thiazolo estrone hybrid heterocycles, Steroids 82 (2014) 29–37, https://doi.org/10.1016/j.steroids.2014.01.003.
[27] L.-H. Huang, Y.-F. Zheng, C.-J. Song, Y.-G. Wang, Z.-Y. Xie, Y.-W. Lai, Y.-Z. Lu, H.-M. Liu, Synthesis of novel D-ring fused 7′-aryl-androstano[17,16-*d*][1,2,4]triazolo[1,5-*a*]pyrimidines, Steroids 77 (2012) 367–374, https://doi.org/10.1016/j.steroids.2011.12.012.
[28] P. Saikia, P.P. Kaishap, R. Prakash, K. Shekarrao, S. Gogoi, R.C. Boruah, R. C. A facile one-pot synthesis of 7-substituted pyrazolo[1,5-*a*]pyrimidines by base induced three-component reaction, Tetrahedron Lett. 55 (2014) 3896–3900, https://doi.org/10.1016/j.tetlet.2014.05.021.
[29] I. Bartonkova, A. Novotna, Z. Dvorak, Novel stably transfected human reporter cell line AIZ-AR as a tool for an assessment of human androgen receptor transcriptional activity, PLoS One 10 (2015), e0121316, https://doi.org/10.1371/journal.pone.0121316.
[30] J. Shaw, M. Leveridge, C. Norling, J. Karén, D.M. Molina, D. O'Neill, J.E. Dowling, P. Davey, S. Cowan, M. Dabrowski, M. Main, D. Gianni, Determining direct binders of the androgen receptor using a high-throughput cellular thermal shift assay, Sci. Rep. 8 (2018) 163, https://doi.org/10.1038/s41598-017-18650-x.
[31] S. Lv, Q. Song, G. Chen, E. Cheng, W. Chen, R. Cole, Z. Wu, L.E. Pascal, K. Wang, P. Wipf, J.B. Nelson, Q. Wei, W. Huang, Z. Wang, Regulation and targeting of androgen receptor nuclear localization in castration-resistant prostate cancer, J. Clin. Invest. (2020), https://doi.org/10.1172/JCI141335.
[32] S. Chen, S. Gulla, C. Cai, S.P. Balk, Androgen receptor serine 81 phosphorylation mediates chromatin binding and transcriptional activation, J. Biol. Chem. 287 (2012) 8571–8583, https://doi.org/10.1074/jbc.M111.325290.
[33] Z. Yu, C. Cai, S. Gao, N.I. Simon, H.C. Shen, S.P. Balk, Galeterone prevents androgen receptor binding to chromatin and enhances degradation of mutant androgen receptor, Clin. Cancer Res. 20 (2014) 4075–4085, https://doi.org/10.1158/1078-0432.CCR-14-0292.
[34] Z. Wu, K. Wang, Z. Yang, L.E. Pascal, J.B. Nelson, K. Takubo, P. Wipf, Z. Wang, A novel androgen receptor antagonist JJ-450 inhibits enzalutamide-resistant mutant ARF876L nuclear import and function, Prostate 80 (2020) 319–328, https://doi.org/10.1002/pros.23945.
[35] C. Tran, S. Ouk, N.J. Clegg, Y. Chen, P.A. Watson, V. Arora, J. Wongvipat, P. M. Smith-Jones, D. Yoo, A. Kwon, T. Wasielewska, D. Welsbie, C.D. Chen, C. S. Higano, T.M. Beer, D.T. Hung, H.I. Scher, M.E. Jung, C.L. Sawyers, Development of a second-generation antiandrogen for treatment of advanced prostate cancer, Science 324 (2009) 787–790, https://doi.org/10.1126/science.1168175.
[36] E. Estébanez-Perpiñá, L.A. Arnold, P. Nguyen, E.D. Rodrigues, E. Mar, R. Bateman, R.J. Fletterick, A surface on the androgen receptor that allosterically regulates coactivator binding, Proc. Natl. Acad. Sci. 104 (2007) 16074–16079, https://doi.org/10.1073/pnas.0708036104.
[37] O. Trott, A.J. Olson, AutoDock Vina: Improving the speed and accuracy of docking with a new scoring function, efficient optimization, and multithreading, J. Comput. Chem. 31 (2010) 455–461, https://doi.org/10.1002/jcc.21334.
[38] G.M. Morris, R. Huey, W. Lindstrom, M.F. Sanner, R.K. Belew, D.S. Goodsell, A. J. Olson, AutoDock4 and AutoDockTools4: automated docking with selective receptor flexibility, J. Comput. Chem. 30 (2009) 2785–2791, https://doi.org/10.1002/jcc.21256.
[39] T. Higashi, Numerical Absorption Correction, NUMABS, 2002.

[40] CrystalClear S.M. 1.4.0 Rigaku/MSC Inc., 2008.
[41] SHELXL-2013 Program for Crystal Structure Solution, University of Göttingen, Germany, 2013.
[42] L.J. Farrugia, WinGX and ORTEP for Windows: an update, J. Appl. Crystallogr. 45 (2012) 849–854, https://doi.org/10.1107/S0021889812029111.
[43] A.L. Spek, Single-crystal structure validation with the program PLATON, J. Appl. Crystallogr. 36 (2003) 7–13, https://doi.org/10.1107/S0021889802022112.
[44] C.F. Macrae, P.R. Edgington, P. McCabe, E. Pidcock, G.P. Shields, R. Taylor, M. Towler, J. van De Streek, Mercury: visualization and analysis of crystal structures, J. Appl. Crystallogr. 39 (2006) 453–457, https://doi.org/10.1107/S002188980600731X.
[45] F.H. Allen, O. Johnson, G.P. Shields, B.R. Smith, M. Towler, CIF applications. XV. enCIFer : a program for viewing, editing and visualizing CIFs, J. Applied Crystallogr. 37 (2004) 335–338, https://doi.org/10.1107/S0021889804003528.